

FINAL PUBLISHABLE JRP REPORT

JRP-Contract number	IND58	
JRP short name	6DoF	
JRP full title	Metrology for movement and positioning in six degrees of freedom	
Version numbers of latest contracted Annex Ia and Annex Ib against which the assessment will be made	Annex Ia:	V1.0
	Annex Ib:	V1.0
Period covered (dates)	From 01 June 2013	To 31 May 2016
JRP-Coordinator	Jens Flügge	
Name, title, organisation	PTB	
Tel:	+49 531 592 5200	
Email:	jens.fluegge@ptb.de	
JRP website address	http://www.ptb.de/emrp/ind58-home.html	
Other JRP-Partners	CMI, Czech Republic	
Short name, country	LNE, France	
	METAS, Switzerland	
	NPL, United Kingdom	
REG1-Researcher (associated Home Organisation)	Josef Lazar ISI	Start date: 1 June 2013 Duration: 21 months
REG2-Researcher (associated Home Organisation)	Eberhard Manske TU-Ilmenau	Start date: 1 Feb 2014 Duration: 21 months
REG3-Researcher (associated Home Organisation)	Nataliya-Vorbringer- Dorozhovets	Start date: 1 May 2014 Duration: 19 months
REG4-Researcher (associated Home Organisation)	TU-Ilmenau Loren Picco Uni Bristol	Start date: 1 Nov 2013 Duration: 31 months

Report Status: PU Public



TABLE OF CONTENTS

1	Executive Summary	3
2	Project context, rationale and objectives.....	4
3	Research results	6
4	Actual and potential impact	38
5	Website address and contact details	42
6	List of publications.....	42

1 Executive Summary

Introduction

This project developed approaches for measuring positioning systems over measurement ranges from nanometres to hundreds of millimetres in all six degrees of freedom (6DoF). The project developed new measurement equipment, facilities, modelling approaches, and standardised procedures, which can be used by a range of European industries to enhance their precision engineering capabilities to develop higher-performance, internationally competitive products.

The Problem

Improved positioning control is needed across a range of applications, from the nano-scale (metrology frames for Atomic Force Microscopy (AFM)) and micro-scale (Coordinate Measuring Machine (CMM), tomography stages) to mechatronics positioning in automotive and aerospace systems. It includes traditional Cartesian motion systems, as well as more general positioning devices (hexapods, goniometers).

Tracability beyond 1-D metrology requires the use of self-calibration methods, which are time consuming and error prone due to differences in the mounting of measurement objects, which causes changes by bendings in the tool structure and the measurement objects themselves. For hexapods so far no traceable calibration services are available over the full motion range. The use of AFM is additionally limited due to the long measurement times necessary in common AFM and the low metrology quality of high speed AFM.

The Solution

In the project a new deflectometric method has been used to determine the topography of a mirror for straightness measurements. The method has been experimentally proved by implementation on a high performance length comparator at PTB by comparison with other common methods like self-calibration by rotation and shift of the measurement object, external calibration of the mirrors and straightness interferometers.

For the calibration of Hexapods a new calibration method using three balls on the hexapod measured by a coordinate measurement machine was developed together with a mathematical method to use the measurement values to correct the errors of the hexapod.

To improve high speed AFM measurements a testbed for offline correction of nano-positioning devices has been set up, metrology has been added for online corrections as well as investigations of tip wear and smart scanning strategies have been implemented in an open AFM data processing software.

Impact

The results of the project have been disseminated in 27 published papers, 48 talks and posters at conferences, 2 workshops and 12 presentations at companies. Additionally, the project outcomes have been presented to ISO and VDI standard committees in the areas of coordinate- and nano-metrology as well as to the EURAMET technical committee for length.

The most important outcome of the project are new measurement services, now provided by the NMIs involved. These new services includes:

- o PTB can now supply a calibration service for calibrations of combined length and straightness encoders like Heidenhain 1D+ Encoders, and straightness interferometers with uncertainties in the nano-meter region using the Traceable Multi Sensor method for deflectometric measurement of topography (TMS). Globally, these calibrations were previously only available with uncertainties more than 10 times larger. Some companies are already waiting for this service on line scales to be implemented.

- METAS will for the first time provide a calibration service for six degrees of freedom (DoF) stages with large angular motion axes like Hexapods or stacked linear and rotational axes on CMMs over the whole motion range. This calibration service will reduce the effort and therefore cost for the instrumentation manufacturers to establish the traceability required for quality management. Due to the modelling effort of METAS this data can directly be used to improve the positioning accuracy of the calibrated stages.
- NPL now supplies calibration services for nano positioning stages for device manufacturers as well as for end users, which can also use the supplied measurement data for corrections using the software GWYDDION.
- PTB can supply samples with mono atomic flat surfaces up to 200 μm as standard for straightness measurements at nano positioning devices

Project partners and stakeholders benefit by getting the first calibrations using the developed setups.

The stabilised laser developed by ISI has been used in a commercial product and the 6-DoF interferometer has been presented at trade exhibitions to check for a potential commercialisation.

2 Project context, rationale and objectives

Need for the project

Mechatronic motion systems are the basis of most production systems ranging from tool machines for wafer scanners in semiconductor circuit production to robotic applications and associated measurement equipment like coordinate measuring machines and scanning probe microscopes. Positioning to the required precision is challenging under dynamically changing and possibly harsh conditions. A trade-off has to be established in being both fast and accurate. Recent European and national strategy and roadmap documents have identified these needs.

Improved positioning control is needed across a range applications, from the nano-scale (metrology frames for AFM) and micro-scale (CMM, tomography stages) to mechatronics positioning in automotive and aerospace systems. It includes traditional Cartesian motion systems, as well as more general positioning devices (hexapods, goniometers). Similarly rich is the spectrum of required accuracies (sub-nm to metre scale uncertainties), dynamics (fast microscopy MHz-scale scanning to low frequency mHz-scale noise spectra of astronomy instrumentation), and simultaneous multi-axes measurement and control. Selection and number of the targeted DoF, measurement range, uncertainty and temporal dynamics depend on the specific applications and the actual on-site ambient conditions.

Increasingly, positioning systems require precision and accuracy not only in the main motion directions but in several, if not all, translational and rotational DoF to allow production with low tolerances. Fast manufacturing processes or dynamic applications give rise to a need for simultaneous measurement and control. Sequential alternation between distinct measurement configurations negatively affects down-time in production and hence costs. A specific challenge is the development of measurement systems for simultaneous measurement of six degrees of freedom with the same levels of precision and accuracy as have been established for single DoF measurements. Additionally, single DoF measurement systems will need a reduction in measurement uncertainties to meet future demands.

While both translation and angle metrology for one dimensional movements are well developed technologies, the combination of multiple axes requires more sophisticated methods for characterisation of the movement. In Cartesian coordinates it is necessary to deal with orthogonality of the measurement systems, the crosstalk to other motion directions, for example in interferometric systems by topography deviations of mirrors. Even more complicated is the characterisation of systems with large angular motion as combinations of angular and linear axes or hexapods. Sophisticated schemes for self-calibration have been developed, which require further validation and measurement uncertainty analysis at the nanometre level.

Error mapping of stages is a practical possibility for more accurate positioning metrology at all levels, reducing effort and costs. In mechatronics applications this includes dynamic error budgeting, taking into

account dynamic and thermal deformations. For nanometrology and in particular AFM metrology, point by point error mapping enables a calculation to be made of local uncertainties for position and other terms that are dependent on position such as surface texture parameters. In recent years there has been a growth in the development of high speed AFMs working at video rate. These can be used for the examination of live processes particularly in the field of biology and medicine and have been imaging things such as the decay of dental enamel. The translation stages used in these AFMs require a high bandwidth and are devoid of any intrinsic metrology. Introducing metrology to High Speed AFM would allow it to be used to obtain quantitative data.

Progress beyond the state of the art

Many methods and instrumentation have been developed for the measurement of motion in all six degrees of freedom as well as for subsystems. While most industrial positioning systems implement grating encoders or, for short range applications, capacitive sensors, this JRP focuses on validation and uncertainty analysis of measurement methods for motion systems with accuracy down to the nm level. It will therefore mainly make use of interferometer systems because of their inherent traceability and will make improvements in several key areas of interferometry.

The high resolution of Fabry-Perot interferometry provides an excellent tool for sensor calibration and for fundamental metrology in the SI. Furthermore, optical interferometry supports fast, dynamic measurements. In practice, the achievable measurement uncertainty is limited due to variable ambient conditions, such as air refractive index, thermal expansion, nonlinearity and alignment errors. Whereas commercial instrumentation is thus limited to nanometre uncertainty (notwithstanding potential picometre sensitivity), NMI work is in progress toward sub-nm uncertainty for ultra-precision applications. This can only be achieved in highly controlled conditions that account for balanced optical beam configuration, in-situ air refractive index compensation, exceptional laboratory stability, optimal artefact orientation, and referencing to primary optical frequency standards or X-ray interferometers. These implementations are typically restricted to a single translation axis and limited dynamics.

To measure all six degrees of freedom with one interface by laser interferometry currently requires complex optics and a large number of components. Therefore it is common to measure the behaviour of stages, e.g. in tool machines, sequentially. This requires much time for the readjustment of the interferometers. Recently, a laser interferometer has been developed which uses Charge-coupled devices (CCD) for the acquisition of interferograms and Field Programmable Gate Array (FPGA) for data analysis with update times in the kHz range. By separate analysis of different regions of the CCD sensors multiple interferometer axes can be simultaneously measured with simple optical components. Using tuneable laser diodes stabilised by mechanical reference will reduce costs and allow for a tracking of the refractive index of air, where commonly additional interferometer axes have to be used as, for example, in mask metrology machines.

A crucial problem in multi-axes interferometry is the influence of the mirror topography. Traditionally, error separation techniques are used but they are time consuming and limited in accuracy by the reproducibility of the mounting conditions of mirrors and measurement objects. Deflectometry is already in use for the measurement of topographies of especially large mirrors or gratings, as used in electron storage rings or X-ray free electron lasers. The technique can be adapted to measure straightness of positioning systems. The deflectometric systems have the potential for sub-nm uncertainties which corresponds to an improvement of more than a magnitude compared to published measurement uncertainties. To achieve the sub-nanometre level with an experimental setup and to obtain comparable results with other setups in the sub-nm range are still real challenges. A more detailed analysis of measurement uncertainties based on experimental results is required, which will also allow for self-calibration methods for nanometre uncertainties. The use of interferometers for the measurement of straightness is well established. Their resolution is limited by the angle between the two interferometer beams, which is limited by the size of the interferometer setup. Therefore small-sized interferometers are mainly in use for tool machines with limited accuracies. With the use of recently developed phase measurement electronics with interpolation factors of 100,000 and optical designs which minimise interpolation nonlinearities, it is possible to achieve nm level uncertainties with small angles and therefore also to reduce the influence of the refractive index of air.

A detailed measurement uncertainty analysis and experimental comparisons of different measurement techniques will enable a better understanding of the limits of precision of motion systems and will help with the identification of appropriate tools for practical motion applications.

Scanning probe microscopes like AFMs usually collect data quite slowly, since single points are measured while a rectangular array is raster scanned with a frame rate of typically 0.01 Hz. For metrology systems, this represents a significant bottleneck as the position of each point in a matrix needs to be reached, stabilised and measured with sufficient precision. Even for systems that do not perform stabilisation at each point, at the end of scanning the data are usually re-sampled onto a regular grid as the data processing software is not able to treat non-equidistant data properly. This is a significant waste of time, data and effort. In the real world information is not spaced equally on the sample surface. There are regions containing more information (e.g. edges) and less information (flat areas). The goal is to acquire data faster with adaptive sampling, depending on the information density. This saves a lot of time and memory resources. Moreover, there is no need for scanning in regular line-by-line patterns, which can instead use innovative scanning strategies, based on prior knowledge, that best fit the corresponding measurement task. By increasing scanning speed significantly we can reach many novel fields of AFM applications. Using adaptive scanning is moreover a necessary step for bridging the gap between AFMs and micro- and nano- coordinate measuring machines.

Scientific and technical objectives

The project focuses on the calibration of motion systems with challenging uncertainty requirements and the development of methods for analysing the associated uncertainty and error mapping for real time corrections. Different approaches and instrumentation for measuring six degrees of freedom motions as well as important aspects like straightness and orthogonality will be analysed and compared. Additionally, the project aims to improve nano-positioning systems for the relevant high-tech fields of the future through novel hardware technology, optimised sensor and actuator components and optimised measurement and control strategies for high speed AFM.

The high-level objectives are:

- *Determination of the straightness of motion with an accuracy of less than 10 nanometers.* The project will implement a deflectometric method using three parallel interferometers and compare the results with other optimised instruments and methods.
- *Development of a compact interferometer to simultaneously measure all six degrees of freedom from one interface.* The goal of the project is the development of a 6DoF-interferometer with a relative length measurement uncertainty in the 10^{-7} region respectively for short length a noise level below 10 nm.
- *Implementation of methods for the characterisation of motion systems with large angular motion like hexapods or stacked systems with mixed angular and linear motion axes.* Characterisation of the motion in six degrees of freedom by step-by-step measurements of reference points will be done with a coordinate measuring machine and compared with laser tracer techniques.
- *Calibration and error mapping in six degrees of freedom of nanopositioning stages regarding positioning errors, angular deviations, straightness of motion and orthogonality.* This includes the development of a high precision low cost interferometer capable of measuring six axes, setting up a test bed for nanopositioning using conventional interferometers and testing sensors.
- *Improvement of the measurement speed of AFM to allow measurements of larger areas and to reduce drift in the instrumentation.*

3 Research results

These results are presented on an objective by objective basis, each section ending with a brief conclusion outlining the new capabilities, materials and insights generated from the research.

3.1 Determination of the straightness of motion with an accuracy of less than 10 nanometers.

Introduction

Beyond one dimension interferometry has to deal with mirror topography issues caused by polishing processes and bending during the mounting operation. Commonly used error separation methods based on rotation and shift of the measurement objects are limited by the reproducibility of the object mounting. Additionally the object cannot in every case be shifted. Therefore a new deflectometric measurement principle has been developed.

To set up the deflectometric straightness measurement with accuracies in the nanometer range, a very stable base measurement machine is necessary. Therefore, the PTB Nanometer Comparator (NMK) was chosen to implement the TMS method with three parallel interferometers and to perform comparison measurements with other established straightness measurement principles including self-calibration methods, external calibration by Fizeau interferometer or straightness interferometer, which generated a large constructive effort. The main parts necessary to implement TMS was a system of three parallel high resolution heterodyne interferometers and a high-quality measurement mirror polished to a Zerodur tray to allow for a stable connection between the measurement object and the mirror. After finishing the hardware PTB and TUIL performed the comparison measurements in cooperation on the comparator. The mirror topography has also been measured externally by a Fizeau interferometer in sequential overlapping steps.

As the NMK is a one dimensional measurement tool orthogonality cannot be determined this way. Therefore, a prototype 2-D Nano-Measurement Machine (NMM) at TUIL was used to perform additional experiments. Measurement methods applied to a 2-D encoder have been external calibration of the L-shaped mirror, error separation and multilateration measurement. Due to interferometry in air and the larger signal period of the encoder, the results are not direct comparable to the NMK results.

Upgrade of the Nanometer Comparator

The basic components of the Nanometer Comparator are schematically illustrated in Figure 1. The distance of structures on a scale were compared with the wavelength of a frequency-doubled Nd:YAG laser. The scale was placed on the measurement slide and moved relatively to the bridge on which the encoder head was mounted. This relative movement and the related angular deviations were measured with the long-range X-interferometer and two angle interferometers. In order to reduce the influence of refractive index variations the X-interferometer as well as the yaw- and pitch-interferometer were working in an evacuated environment with a pressure of 2 Pa. The light of each input beam had been frequency-shifted by means of acousto-optic modulators (AOM) and was transferred from the laser to the heterodyne interferometers using an individual polarization-maintaining fibre. This spatial separation of input beams reduces periodic nonlinearities caused by frequency mixing. The periodic nonlinearities of the X-interferometer were below 15 pm without any additional corrections. Hence a standard uncertainty of the X-interferometer of 0.16 nm was achieved.

The measurement slide as well as the bellows slide were moved by linear drives. Both slides were equipped with air bearings for a frictionless movement over the granite base. The angle variations between the bridge and the moving slide were minimised using the angle interferometer signals in a closed loop control, regulating the voltage supplied to piezoelectric actuators. These actuators were embedded in the moving slide and were also used to introduce angle variations to adjust the Abbe offset of the encoder system relative to the interferometers. The angle interferometers were calibrated using an autocollimator as transfer standard. A length dependent deviation of the angle interferometers was observed, leading to a position dependent uncertainty of the yaw-interferometer of 421 nrad/m.

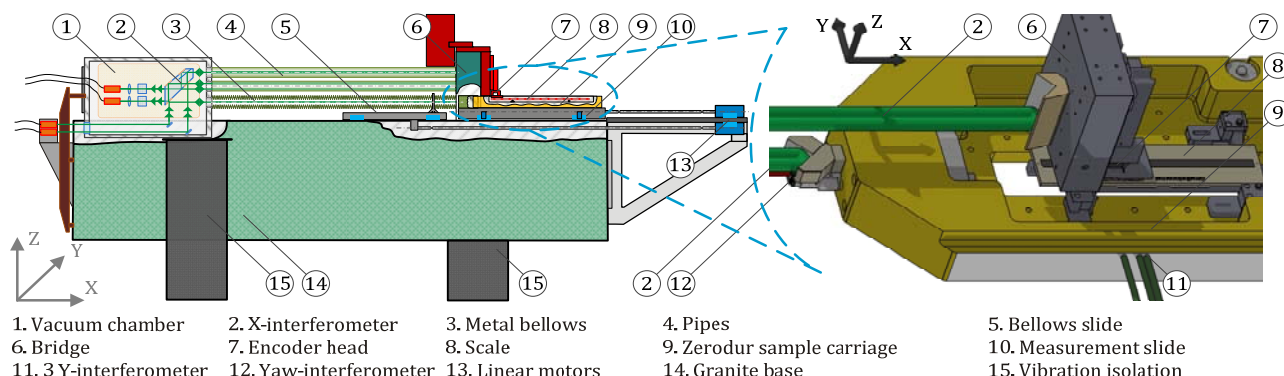


Figure 1. Schematic diagram of basic components of the Nanometer Comparator and the arrangement of the measurement systems

Three parallel heterodyne interferometers were realised as shown in figure 2, based on the same principle like the length interferometer using one glass structure. The usage of a plane-parallel plate as beam splitter resulted in equal vertical gaps and equal path differences between the beams 1 and 2 and the beams 3 and 4. Therefore, a roll angle variation of the bridge, fulfilling Abbe's criteria with an adequate positioning of the scale, as well as homogeneous thermal expansion of the glass were intrinsically compensated. The interferometer design allows for a minimal dead path with an adequately placed reference mirror. The dead paths of the interferometers were determined to be below 0.6 mm by frequency variations of the laser. The position of the reference mirror coplanar with the moving mirror and the integrated central glass prism resulted in minimal beam paths through air and a minimal influence of gradients of its refractive index. The refractive index was corrected by monitoring the ambient conditions and using Edlén's formulae.

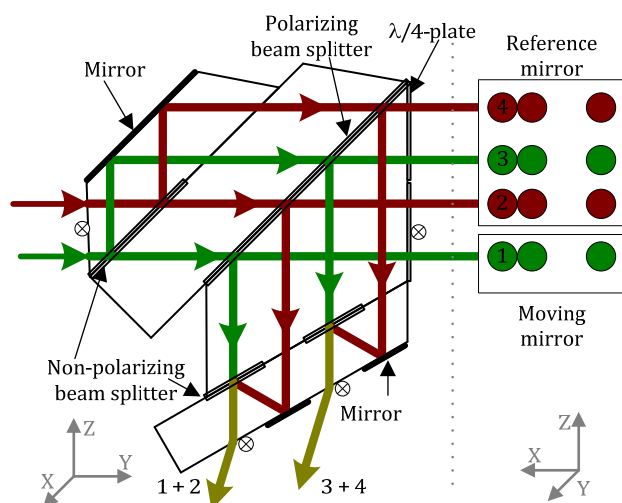


Figure 2. Beam path through the Y-interferometer optics, red beam had a frequency-shift of 78.4375 MHz and the green one of 80 MHz.

The influence of potential reflections from the optical components was minimized by introducing a small tilt to all of them, including the interferometer optics. The lenses in front of the photodiodes in combination with a limited active area worked as a spatial filter for multi-reflected beams with different incidence angles. The signals with a beat-frequency of 1.5625 MHz were converted with transimpedance amplifiers and acquired by an analogue-to-digital converter board with on-board memory and field-programmable-gate-array (FPGA) chips. A lock-in based phase evaluation was implemented in the FPGA units allowing a data acquisition rate of 48.8 kHz. This board was used to process the signals of all three Y-interferometers and the encoder system simultaneously.

The three Y-interferometers were realised using two plane-parallel plates and a mirror placed in front of the interferometer optics. These plates were coated with NPBS and mirrors to split the incoming beams with different frequencies into three ones each. This separation resulted in three Y-sensors with coprime interspaces in the X-direction. These interspaces were input parameters of the TMS method. By means of a quadrature detector mounted on the moving slide they were determined to be the 23.488 mm between the first and the second Y-interferometer and 34.588 mm between the first and third one.

The standard uncertainties of the three Y-interferometer were different and determined to be $u(Y1)=0.23$ nm, $u(Y2)=0.10$ nm and $u(Y3)=0.03$ nm. They have been dominated by periodic nonlinearities caused by reflections from the photodiodes and the influence of the dead path due to variations of the refractive index of air. The periodic nonlinearities were determined in comparison with the encoder system taking advantage of its different signal period. The uncertainties were considered to be uncorrelated.

For the evaluation of the TMS method for straightness measurements a custom made grating scale of the company Dr. Johannes Heidenhain GmbH was used. The measurement grating with a period of 512 nm, a length (L) of 322 mm and a width of 15 mm was deposited on a Zerodur substrate. The encoder system was chosen as comparison standard, because of its high resolution (5 pm at a bandwidth of 20 kHz) and high reproducibility (<0.2 nm after the subtraction of the linear drift). Its uncertainty contribution caused by periodic nonlinearities was below 7 pm, once the measurement data had been corrected offline. The encoder system was adjusted with an Abbe offset below 38 μm in Z-direction to the Y-interferometers. The first and third Y-interferometer were placed symmetrically to the encoder head in X-direction with an Abbe offset below 80 μm . In both cases the Abbe offset was determined by angle variations of the measurement slide in combination with an autocollimator measuring the angle of the Y-mirror.

Error separation methods for straightness measurements

The measurement data of the three Y-interferometers and the yaw-interferometer were used to determine the topography of the Y-mirror and the horizontal slide straightness error. The measurement process was modelled using a small-angle approximation, which resulted in a system of linear equations, which can only be solved with two additional boundary conditions set to the topography and the systematic sensor errors. Therefore, the TMS method determines the topography and Y-movement only up to an arbitrary straight line. The mirror topography was interpolated with Lagrange polynomials to allow a non-equidistant interspacing between the sensors and measurement points. This interpolation has no effect on the linearity of the equation system, which was solved using a weighted least-squares method. The covariance matrix of the measurement values was used as weight. This matrix was not diagonal, because the length depending error of the yaw-interferometer led to correlated measurement values.

The reconstructed horizontal slide straightness error was subtracted from the measurement values of the encoder system to obtain the straightness deviation of the scale. The main advantage of the TMS method is the simultaneous measurement of mirror topography and straightness while for the reversal method the uncertainty depends on the stability of the mirror topography while rotating and readjusting the scale. Instead of using an angle measurement and a multi-sensor element the slide straightness error can be separated from the straightness deviation of the scale by a reversal method. The scale has to be measured at least in 0° and 180° orientation. In analogy to the rotational shears at the three-flat test or the interspaces of the sensors in the multi-sensor element the lateral resolution of the reconstructed straightness deviation can be increased by multiple shifts of the scale prime to each other.

The average values of the first and third Y-interferometer were directly subtracted from the measurement values of the encoder system. The resulting differences were independent of the slide straightness error and angle variations. They ($S(x)$) were modelled as sum of the straightness deviation of the scale ($G(x)$), the effective Y-mirror topography ($F(x)$) and an unknown straight line ($a \cdot x + b$), which depended on the alignment of the scale and the sample carriage. Shifting the scale in X-direction to another position inside the sample carriage resulted in a different topography ($F(x+d_i)$) and a different straight line. A rotation of the scale by 180° changed the sign of the straightness deviation and their sequence ($-G(L-x)$). For a solvable system of linear equations, at least two measurements with different orientations of the scale and a boundary condition to the topography are needed. Including more measurements to the equation system than needed for an adequate lateral resolution would increase the uncertainty due to sensor noise. The adequate lateral resolution is defined by the transfer function of the sensor given by the beam profile of the Y-interferometer. Similar to the systematic sensor errors at the TMS method the parameter of the unknown straight lines has to be included to the reconstruction in order to receive a unique solution of the equation system. In analogy to the gaps between the sensors at the TMS method the shifts (d_i) of the scale are input parameters for the equation system and were determined using the signal amplitude of the encoder system. In contrast to the TMS method more than one measurement has to be performed and the topography of the Y-mirror has to remain unchanged during these measurements, but it is independent of angle variations.

Results of the straightness measurements

Thirteen series of measurements of the scale were performed. For each series, the scale was measured 14 times, seven times each with forward and backward moving direction of the slide. After each series, the scale was shifted and seven measurements were performed with a 180° orientation. The shifts of the scale were in the same dimension as the distances between the Y-sensors. To reduce boundary effects of the TMS method at positions which had not been measured by all Y-sensors the slide was always moved over at least 360 mm.

The same data was used to apply both error separation methods. In both cases the mirror topography was reconstructed with an interspacing between the reconstruction points of 1 mm, which was smaller than the Y-interferometer beam diameter of 4.1 mm and provided consequently a sufficient spatial resolution.

For each series of measurements the straightness deviation was evaluated 14 times with the TMS method. The repeatability was below 0.1 nm every time, because the slope of the yaw error was constant during one series. The reproducibility was much larger than the repeatability, as shown in Figure 3. The evaluated straightness deviations differed in the range of ± 5 nm from their common mean for the measurements series of the scale in different positions and orientations.

Due to the variation of the yaw error with the initialization of the NMC, there exists no correlation of the deviations with the orientation of the scale. The differences had a parabolic curve progression, correlating with an integration of the length depending error of the yaw-interferometer. The observed variation of the straightness deviation indicated a variation of the slope of the yaw error in the range of ± 730 nrad/m, which is in agreement with former results obtained during the calibration of the yaw-interferometer. On account of the small uncertainties of the Y-interferometers, this effect dominated the uncertainty of the measured straightness deviation using the TMS method. For a single measurement series the standard uncertainty was below 4.2 nm and for the average value of all 13 series, shown in Figure 4, it was below 1.5 nm.

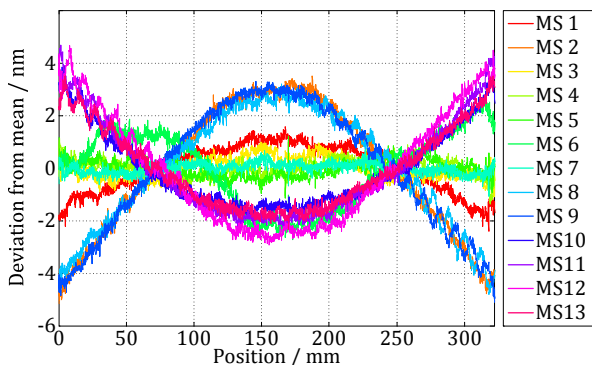


Figure 3: Reproducibility of the straightness measurements with the TMS method; deviations of 13 results with different scale positions and orientations from their common mean.

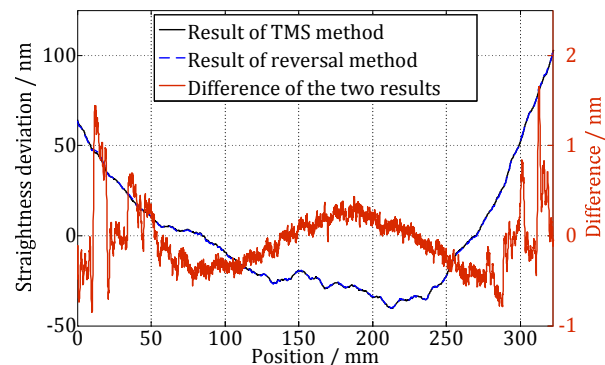


Figure 4. Horizontal straightness deviation of the sample evaluated with the TMS method and the reversal method and their difference.

The reversal method, as performed at the NMC, was independent of yaw-angle variations. But the results of the TMS method had indicated a violation of a basic requirement of the reversal method. The topography of the Y-mirror varied in the range of ± 30 nm between the 13 measurement series. These deformations of the mirror were caused by different thermal expansion coefficients of the sample carriage made of Zerodur and the alignment stages for the scale made of Invar in combination with the small temperature rise during the alignment process of the scale. The evaluated mirror topographies were used to determine the uncertainty of the reversal method. But they had not been used for corrections to have independent results for the two methods. Out of the 13 series of measurements, the combination, yielding to the smallest uncertainty, was chosen for the evaluation of the straightness deviation with the reversal method. Including a higher number of measurements in the equation system can reduce the uncertainty in case of systematic deviations because of compensation effects brought about by the different orientations of the scale. By using 8 out of the 13 measurements a standard uncertainty of 5.2 nm was achieved. The evaluated straightness deviation and the difference to the result of the TMS method are shown in Figure 4. The difference of the two results had a peak-to-valley (PV) value of 2.5 nm, which is in agreement with the uncertainties of both results. The influence of the mirror topography variations can be spotted clearly in the locations of the jump discontinuities at both endings of the difference curve, which correspond to the shifts (d) of the scale. Both methods can be further improved in the future by optimizing the yaw-angle interferometer and the scale mount.

Straightness interferometry

Straightness interferometers are using a splitting element in combination with a straightness reflector realising two beams with an angle relatively to each other and to the moving direction of the slide. Independently whether a grating, wedge prisms or a Wollaston prism is used to split the beams, straightness interferometers are limited by three main error sources: their resolving capability, gradients of the refractive index and the mirror topography of the straightness reflector. Their resolving capability can be improved by

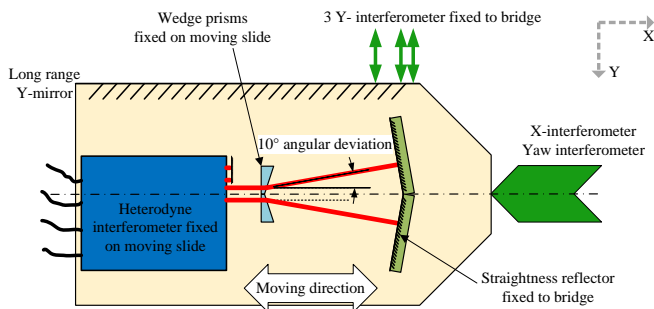


Figure 5: Integration of the straightness interferometer at the Nanometer Comparator for the characterization of its measurement deviations with different wedge prisms.

increasing the angular deviation between the two beams. But an increased beam angle causes a gain of the two other main error sources. Generalities about the optimal configuration do not exist, since the achievable uncertainty depends on the environmental conditions, the mirror topography and the quality of potential error corrections with a reversal method or a characterization of the mirror topography. Furthermore, a straightness reference with a smaller uncertainty is needed to analyze the influence of the different error sources.

The TMS measurements were compared with the measurement results on a straightness interferometer. To setup this straightness interferometer a fiber-fed, heterodyne interferometer with spatially separated input beams, similar to the interferometer described above in 'Upgrade of the Nanometer Comparator' was equipped with two wedge prisms. The interferometer system exhibited periodic nonlinearities below 20 pm and a resolution of 5 pm at a data acquisition rate of 10 kS/s while working as displacement interferometer. The straightness measurements were performed with three different wedge prisms with angular deviations of 2°, 4° and 10°. The system was mounted on the moving slide of the Nanometer Comparator, as shown in figure 5. The different angular deviations result in different phase factors of the straightness interferometer, which were determined in comparison to the Y-interferometers of the Nanometer Comparator during stimulated Y-movements of the slide. These scale factors of 14.293, 7.182 and 2.871 directly define the respective resolving capability and the influence of the mirror topography. Figure 6 illustrates the standard deviation of six straightness measurement repetitions and the systematic measurement deviation of the straightness interferometer caused by the mirror topography. A correction of the mirror topography based on measurements with a Fizeau interferometer was not possible, because the effective topography variation was smaller than the uncertainty of the Fizeau interferometer. Anyhow the standard uncertainty of the straightness interferometer is limited by the effects of the refractive index of air and is large compared to the error separations methods described above.

The TMS measurements were compared with the measurement results on a straightness

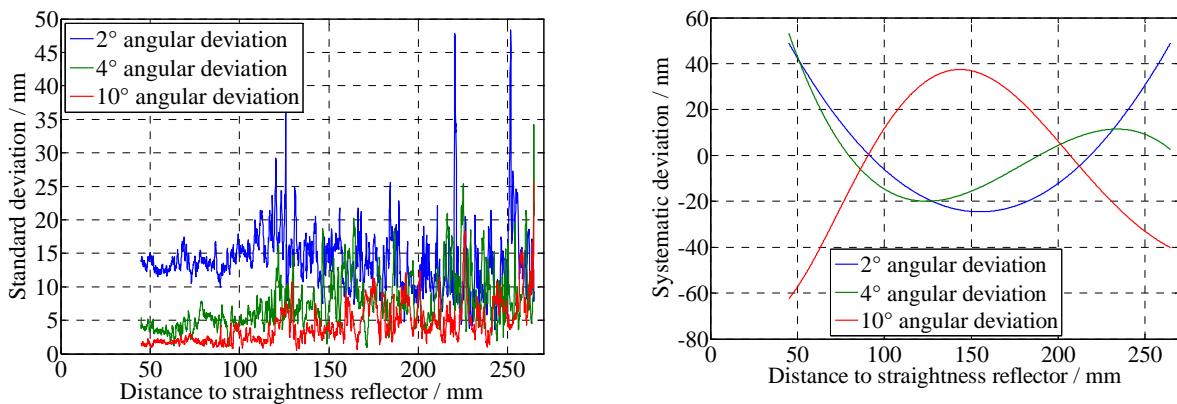


Figure 6: Characterization of a straightness interferometer with different wedge prisms; (left) standard deviation of the measured straightness deviation, (right) Systematic deviation of the straightness interferometer evaluated in comparison to the straightness measurement of the Nanometer Comparator

Straightness and orthogonality measurements at the TUIL prototype Nano Positioning and Measurement Machine

The NPMM-testbed consists of a planar H-structure guiding system with a positioning range of 200 x 200 mm² and a maximum velocity of 30 mm/s. The mirror cube is mounted on the x-axis which is mounted on the y-axis of the machine. A single beam laser interferometer with a resolution of 80 pm measures the y-position. In order of measuring the x-position and the rotation about the z-axis a dual beam interferometer is applied. Figure 7 shows the NPMM-testbed. The position signals are provided to a dSpace rapid control prototyping system which runs the sequence control, trajectory generator as well as the motion control algorithm. The developed model based decoupling control system with dynamic friction compensation allows a positioning accuracy of less than 1 nm. The motor controllers generate the electrical current that actuates the linear drives of each axis. A PC is used for operating the dSpace system, storing measurement data and further evaluation.

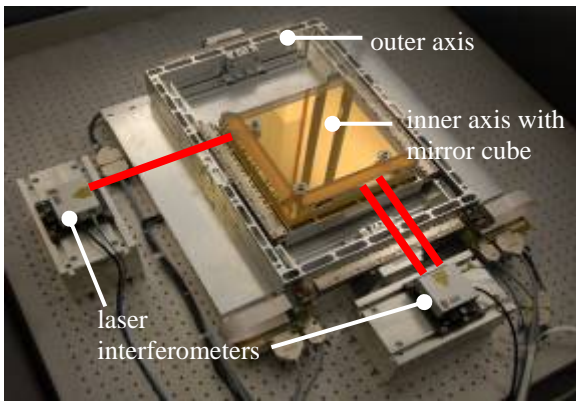


Figure 7: NPMM-testbed

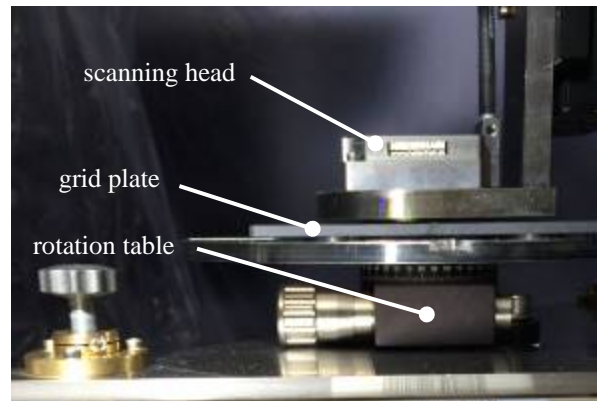


Figure 8: Heidenhain PP281 on the NPMM-testbed

A Heidenhain PP281 two-coordinate encoder was mounted on the NPMM-testbed. The grid plate is carried by a rotation table which is attached to the corner mirror. The scanning head is mounted on the cover plate of the testbed. The mounted encoder system is shown in figure 8. The position signals are decoded by a Heidenhain evaluation electronics and the resulting coordinate positions are transferred to the PC.

The measurement mirror of the NPMM was calibrated by a Zygo Fizeau interferometer using overlapping sequential measurements, which were stitched together. The mirror topography is shown in figure 9

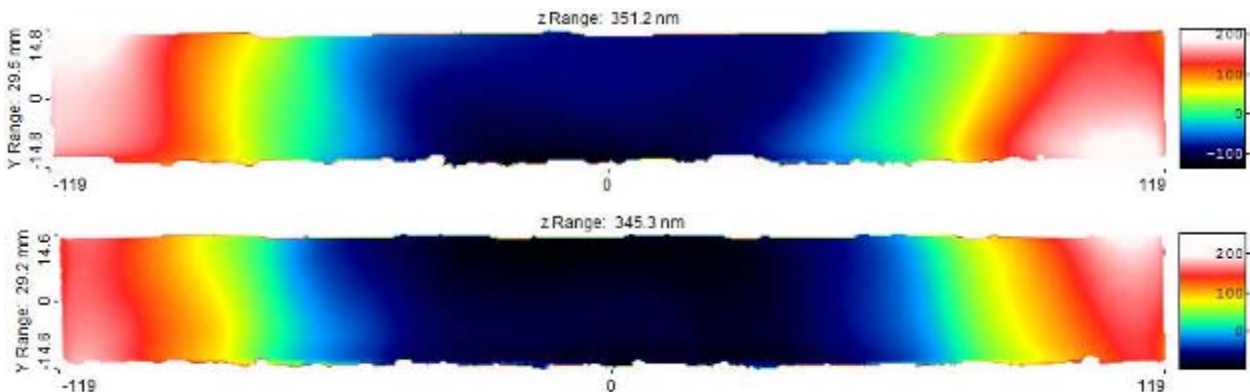


Figure 9: Topography of the NPMM mirror (top: x-axis; bottom: y-axis)

Input quantity	Value / nm
Topography of the reference flat	5
Thermal distortion of the reference flat	0.2
Thermal distortion of the test flat	0.2
Distortion of camera image	1
Overall noise in the camera signal	1
Error in determination of test aperture	0.5
Errors in sizes of phase steps	1
Errors due to collimator aberration	0.5
Expanded Standard Uncertainty (k=2) U	10.68 nm

Table 1: A typical measurement uncertainty budget for interferometric flatness measurement

Together with PTB the measurement uncertainty of the Fizeau interferometer was developed. The main influence quantity with interferometric flatness measurements is the knowledge of the reference flat. The reference flat can be in principle measured against a liquid surface, with the 3-flat-test or with the small angle deflectometry. Measurements against the liquid surface can cause errors due to vibrational and thermal disturbance of the liquid surfaces, the surface of the reference flat

has usually to be coated (when applying a mercury mirror) to get high reflectivity and the measurement can be done only in horizontal orientation. Nevertheless similar or even better results for the calibration of the reference surface can be achieved with a liquid mirror. Small angle deflectometry measures single lines and has typical a rather low spatial frequency resolution of less than 1 mm⁻¹. Thus, the 3-flat test will be often used for measurement of the reference flats at NMIs. The three-flat-test is a self-referencing procedure. Only the accuracy of the alignment of the plates and number of measurements determines this uncertainty. A typical measurement uncertainty budget is given in Table 1. The expanded uncertainties in surface height values at 95% confidence level (coverage factor k=2) is given by approx. 11 nm.

The noise level of the interferometer is mainly caused by refractive index fluctuations and non-repeatability of the guidance. Based on this results it can be concluded, that external calibration of the mirror is a suitable solution for machines using interferometry in air.

The long term stability of Zerodur mirrors repeated older measurements on a flat with 150 mm diameter, performed at PTB over 4 years were re-evaluated. After removing high frequency components the remaining low spatial frequency topographies are used for the determination of the PV value. From the results shown in figure 10 it can be seen, that the changes are smaller than the measurement uncertainty of the Fizeau interferometer.

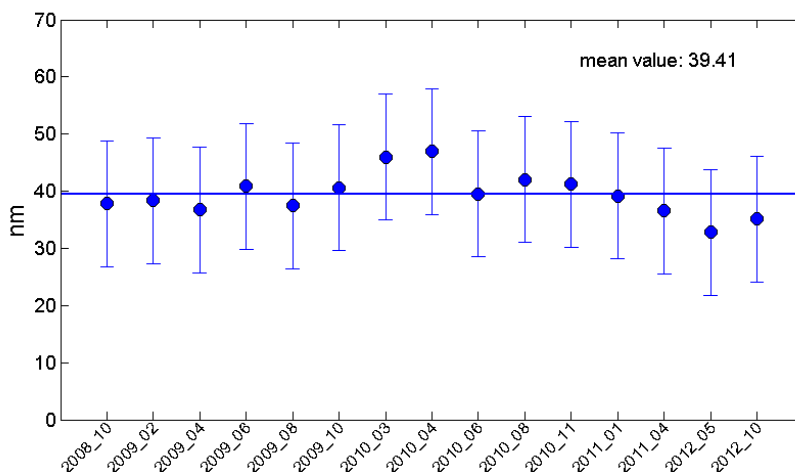


Figure 10: PV value of the low frequency contributions of the 15 PTB control measurements with uncertainty bars (k = 2) for a time period of 4 years

To determine the orthogonality of the mirrors two autocollimators were used, which were adjusted before using a precision right angle prism, with an angle tolerance of 2 arcsec as shown in figure 11. To reduce the uncertainty the prism can be calibrated before using an angle comparator. Due to the topography of the mirror, the angle measured depends on the position of the autocollimator measurements. On the NPMR mirror the combination of three masked measurement points on both arms results in orthogonality deviations between -3.18" and -5.98".

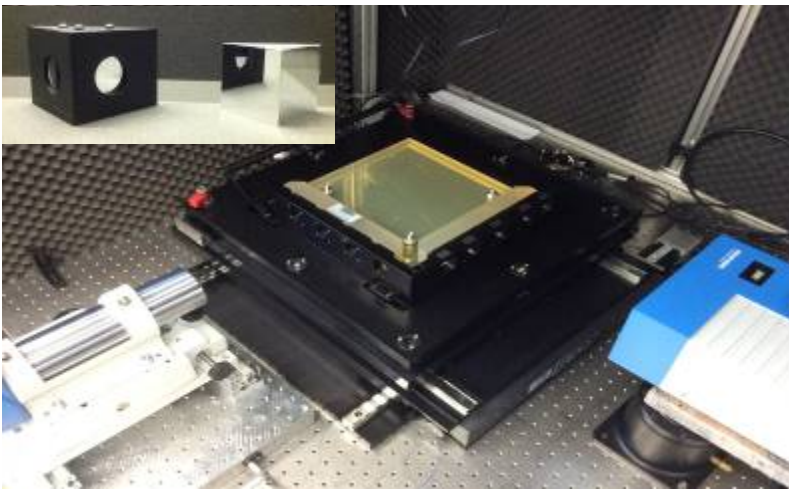


Figure 11: Orthogonality measurement using two autocollimators and a reference cube.

As an alternative method a multilateration with a 3x3 equidistant grid was investigated. The measurement principle is based on distances between multiple points on the grid plate. By rotating the plate the laser beam is always aligned with the movement. This reduces the effect different error sources like drift effects or squareness and straightness errors of the mirror. Using the rotation table the grid plate is rotated in such a way that at least two measurement positions are aligned along the x-axis of the NPM-testbed (Figure 12). 4 shows the first to fourth measurement configuration exemplarily. The rotation is carried on until a complete rotation is completed. The positions

on the dashed lines are measured. This requires the NPM-testbed to only move the x-axis. The y-axis maintains its position.

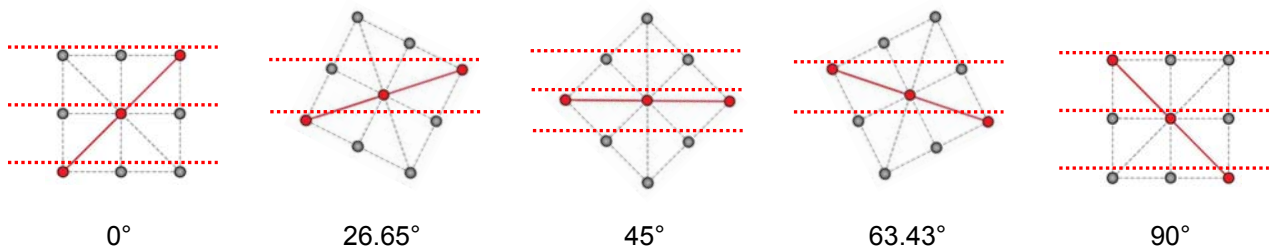


Figure 12: The first four rotations and measurement lines of the multilateration procedure

In contrast to conventional multilateration using image processing the Heidenhain sensor head has to be rotated in the exact same angle as the grid plate. Due to the small number of points the measurement uncertainty of the orthogonality of around 1" is relatively large. To improve the method automatic rotation tables for grid plate and encoder head would be necessary.

Conclusion

A new deflectometric method (TMS) has been implemented to measure straightness online during a measurement process. This reduces time and effort of offline calibration procedures like external calibration procedures or reversal methods. The actual implementation on a high precision length comparator gave superior measurement uncertainty results compared to conventional methods. After removing some limitations of the instrument, found during the project, sub-nm measurement uncertainties will also be possible using TMS. The TMS principle can be adapted on other measurement systems like encoders or capacitive sensors as well and can therefore be used to improve a wide range of measuring and manufacturing tools which use stacked encoder systems.

The work of the project allows PTB to supply a new calibration service for straightness encoder systems, straightness interferometers and in future also tactile measurements with a traceable measurement uncertainty 10 times better than currently available. The mathematical tool developed in the project can also be used to find optimised solutions for 2D and 3D applications.

The project also verifies that for most measurement machines operating with interferometers under atmospheric environments with the associated uncertainties the external calibrations are an appropriate method to compensate topography deviations. The same restrictions are valid for straightness interferometers even with ultra-high resolution phase measurement electronics.

This research presents the results for the project objective, 'Determination of the straightness of motion with an accuracy of less than 10 nanometers and the target of the research has been met.

3.2 Development of a compact interferometer to simultaneously measure all six degrees of freedom from one interface.

Introduction

A high accuracy interferometric 6 degrees of freedom (DoF) measurement system with Ångström resolution for displacement and μrad resolution for angle measurement was developed. The goals of the development were to realise a measurement system which is mobile, robust and as simple as possible. Its main application is the characterisation of the motion axes of high precision machine tools and measurement systems in industrial use where a sub micrometer resolution for the displacement and a μrad resolution for the tilt detection are demanded. Mostly interferometer vendors have systems available measuring length, yaw and tilt angle simultaneously. For measuring straightness, the interferometer optics must be exchanged. During the project an interferometer for 5 DoF has been launched, leaving out the roll angle. The new 6 DoF interferometer is based on a modified homodyne Twyman-Green interferometer concept. It uses a novel signal acquisition and processing approach whereby a spatial interferogram is captured by a CMOS camera and the registered fringe pattern is transformed into its frequency spectrum. The spectral representation of a movement of e.g. a positioning stage is analyzed for its major components: the phase information directly correlates with the displacement of the stage, while a possible rotational motion causes a shift in the frequency spectrum. The developed compact 6 DoF head uses multiple rays in parallel to detect x-y-z displacements and roll-pitch-yaw movements.

The interferometer concept

The key component of the system, the interferometer unit, resembles a bare-minimum Twyman-Green interferometer consisting of a collimator for light coupling, a 50/50 beam splitter, the reference mirror, the measurement mirror and an image sensor (Figure 13). The restriction to a minimum number of optical components reduces errors induced by multipath reflections and wave front aberrations, saves cost, enables miniaturisation and eases adjustment.

In contrast to to a standard interferometer the presented system utilises image sensors to capture the interferogram. The reference mirror and the measurement mirror are adjusted in a way that a fringe pattern is projected onto the sensor. The interferogram consists of a spatial sinusoidal signal whose frequency per unit length depends on the tilt between the reference mirror and the measurement mirror as well as the wavelength of the light source.

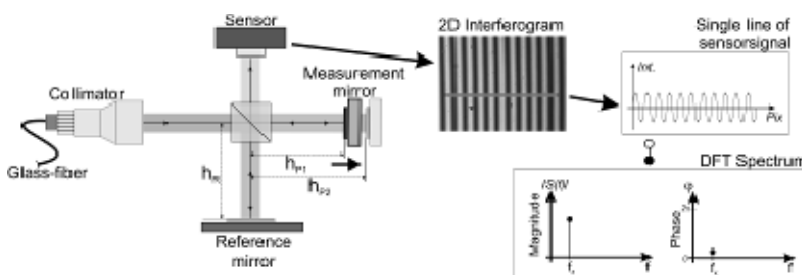


Figure 13: Schematic diagram of the setup (left). The captured and transformed signal (right).

The changes in this fringe pattern are analyzed for the measurements: if the measurement mirror is moved along the beam axis, the pattern shifts in phase in the case of a tilt of the measurement mirror the pattern undergoes a change in frequency.

The signal acquisition of the fringe patterns is performed by CMOS camera modules (e. g. UI-3060CP Rev.2 with USB 3.0 interface from

IDS). Each module captures two fringe patterns: *camera 1* is responsible for the beams *a* and *b*, *camera 2* for the beams *c* and *d* (see figure 14 right), respectively.

The present system uses a personal computer for the signal acquisition and signal processing. A *LabView* based software was developed for the system control: it includes a camera configuration module, a measurement signal definition part and a signal processing unit.

Optical setup for multiple degrees of freedom (DoF)

The developed system is a combination of a length, angle and straightness interferometer based on the interferometer principle described above. The device is able to measure lateral motion in the range of centimeters and angles of up to multiple mrad simultaneously.

The system follows a modular concept. It consists of four separated components: the light source unit, the fixed measurement head, the moveable measurement mirror and the signal processing unit. As a light source a 10 mW cylindrical HeNe laser from Qioptiq is used. The emitted laser beam is divided into four

parts with the same power each by using a fiber optic coupler (FCQ632-FC 1 x 4 single mode fiber coupler from ThorLabs) and connected to four collimators installed in the measurement head unit. By this four independent collimated beams are created and each beam can be used as an independent measurement axis. After system assembly and adjustment the beams have the following properties (see Fig.14 left): beam **a** runs parallel to the **z** axis and perpendicular to the measurement mirror surface plane **A**; beam **c** runs parallel to the **z** axis too but is shifted with respect to the beam **a** in the **x** and **y** direction by the same distance; beam **b** is orientated in the same **yz** plane as beam **a** but tilted along the **x** axis to be perpendicular to plane **B** of the measurement mirror; beam **d** is situated in the same **xz** plane as beam **c** but tilted along the **y** axis to be perpendicular to plane **C** of the measurement mirror.

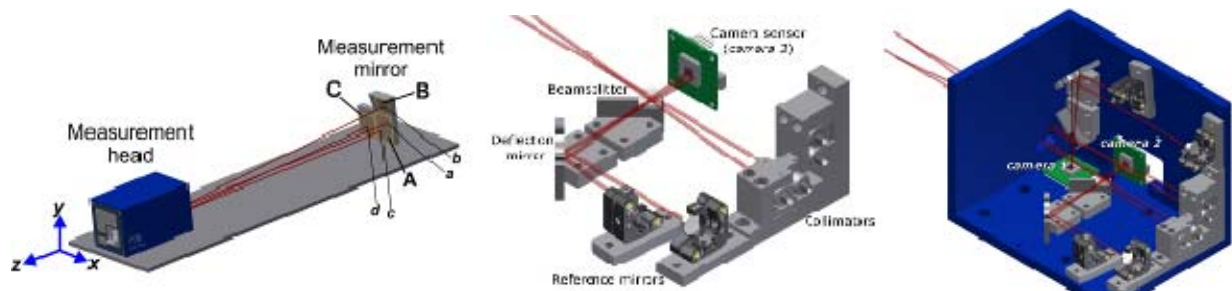


Figure 14: System design with the measurement head and the movable measurement mirror unit (left), the optical setup for the **xz** plane (beams **c** and **d**), which is located inside the measurement head (middle) and the complete measurement head (right)

To create a measurement signal (according to the fringe pattern in figure 14) four independent reference mirrors are used (see figure 14 right). By tilting the reference mirrors the orientation of the fringe pattern can be adjusted: to get nearly uniform tilt sensitivities in each tilt direction a horizontal fringe pattern orientation is arranged for beams **a** and **b**, while a vertically directed fringe pattern is arranged for beams **c** and **d**.

Measurement system characterization

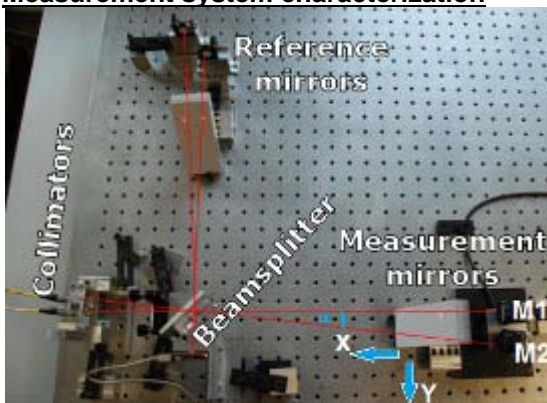


Figure 15: Test setup

Initial test measurements were done to characterise the interferometer performance. These characterizations have been done on an optical bench as shown in figure 15 with measurement length up to some 100 mm under standard laboratory conditions.

To determine the noise level and the resolution limit of the system we removed the scanning unit and fixed the measurement mirror unit directly to the breadboard. A noise level for the position and angle values in the Ångström and in the µrad range was obtained (p-v values), respectively (Figure 16). Because of the environmental characteristics (thermal and mechanical instability, air turbulence etc.) during the test, drifts have been observed, being in the range of less than 10 nm. These unstable conditions were kept unchanged because they are similar

to the expected measurement conditions for the final application of the measurement system. For the straightness interferometers the deviations are by a factor of five larger, because the difference in the refractive indices between the two interferometer beams are multiplied by the factor of lower sensitivity as shown in figure 17.

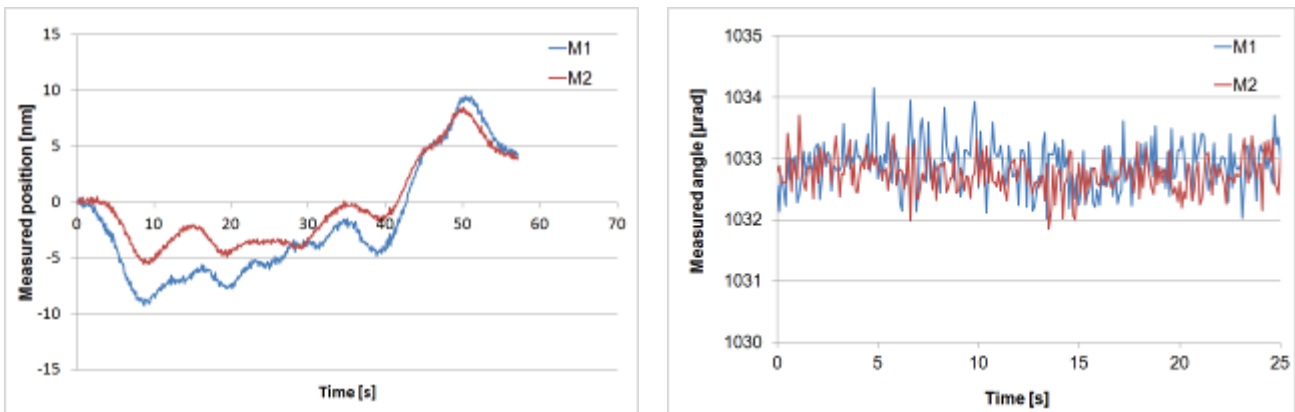


Figure 16: Position (left) and angle (right) results with fixed mirrors to determine noise

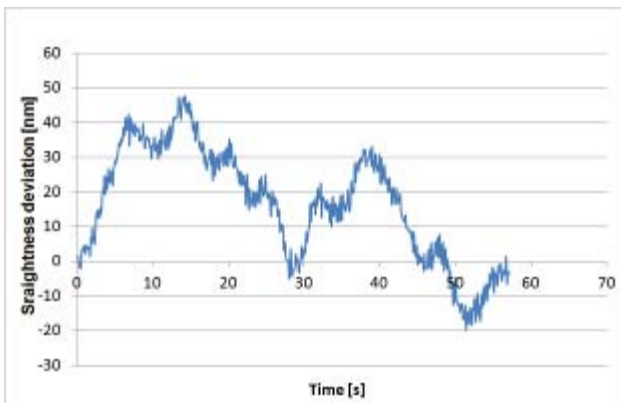


Figure 17: Straightness results with fixed mirrors

Distributed Bragg Reflector Light Source

Within the project new laser sources for interferometry have been investigated and tested by ISI. For the 6-DoF interferometer a compact stabilised laser with a high output level at a low price is necessary as a light source, which allows for an easily transportable interferometer system with a low noise level. We concentrated on semiconductor lasers operating in a single-frequency regime at a wavelength close to He-Ne laser traditionally used for metrological applications ($\lambda=632.9$ nm in vacuum). The aim was to verify whether such a system could be used as an alternative to the He-Ne laser while yielding wider optical frequency tuning range, higher output power and high frequency modulation capability. The full laser system had to be frequency stabilised and designed for operation either for homodyne detection (single frequency output) or for heterodyne detection (two-frequency output with a stabilisation of the beat frequency).

The heart of the laser system is the Distributed Bragg Reflector (DBR) free-space laser diode in a standard TO-3 package. The temperature controller (TC) in conjunction with the thermal control elements (TH) built into the laser diode package are used to control the diode chip temperature. The injection current is driven by a current controller (CC; built-in to the LH) that allows for externally driven fast-bandwidth current modulation. The CC relies on an ultra low-noise power supply (PS). Both the TC and CC controllers are microprocessor-based systems custom-built at ISI (Figure 18).



Figure 18: Modular rack-frame temperature and current controllers and the TO3 laser head.

Stabilisation of the laser optical frequency was referenced to transitions in molecular iodine. Linear spectroscopy technique is used in conjunction with the first harmonic detection technique. We have measured the basic characteristics of the laser source and then we have compared the performance of the laser system with that of a traditional frequency stabilised He-Ne laser with a series of experimental arrangements similar to those usually found in laser interferometry and displacement metrology applications. A schematic diagram of the setup is shown in Figure 19.

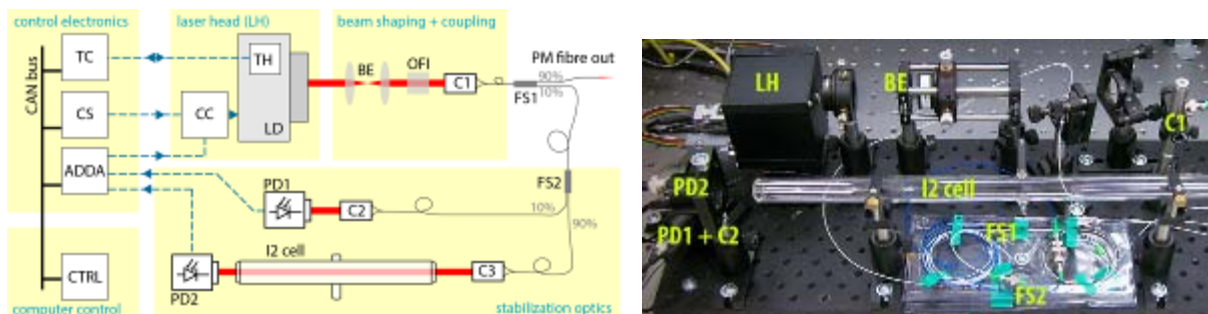


Figure 19. Overview of the laser frequency stabilisation setup and a photo.

The performance of the stabilised laser source have been tested on an interferometric testbed setup using the NPL Plane Mirror Differential Optical Interferometer and have been performed at NPL within a cooperation supported by the project. The optical arrangement is differential, based on Jamin beamsplitter. Figure 20. shows the noise spectra, expressed in the terms of power spectral density, observed within the measurement. It has shown that the most significant contributions to the noise are common for both lasers.

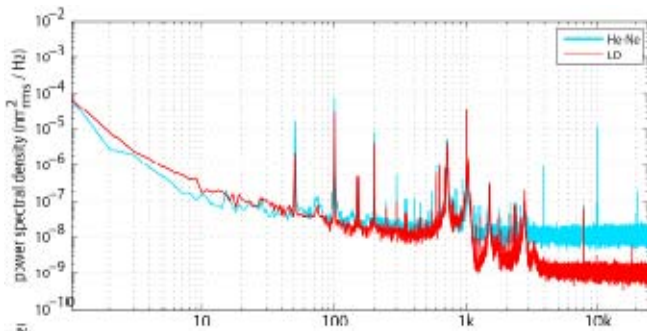


Figure 20: Noise spectra: DBR diode laser v. He-Ne

generating a beat frequency at a PIN photodetector. The stabilisation avoiding a frequency modulation relies on a lock onto a side of a Doppler broadened iodine absorption line. Optical frequency of the DBR1 laser is locked to the iodine absorption line, frequency of DBR2 to a desired reference rf signal from the heterodyne detection system via a fast analog controller. Optical outputs from both lasers are independently fiber coupled for light delivery into the interferometer (Figure 21).

A more complex system exploiting the developed technology and instrumentation mentioned above has been designed to operate in a two-frequency operation with a stabilisation of the optical frequencies and also stabilisation of the rf beat frequency. The design is referring to the needs of a project coordinator, PTB where heterodyne detection of interference signals is needed.

The design consists of two identical DBR semiconductor lasers with control electronics and an optical setup feeding part of one laser output into a reference iodine absorption cell and also

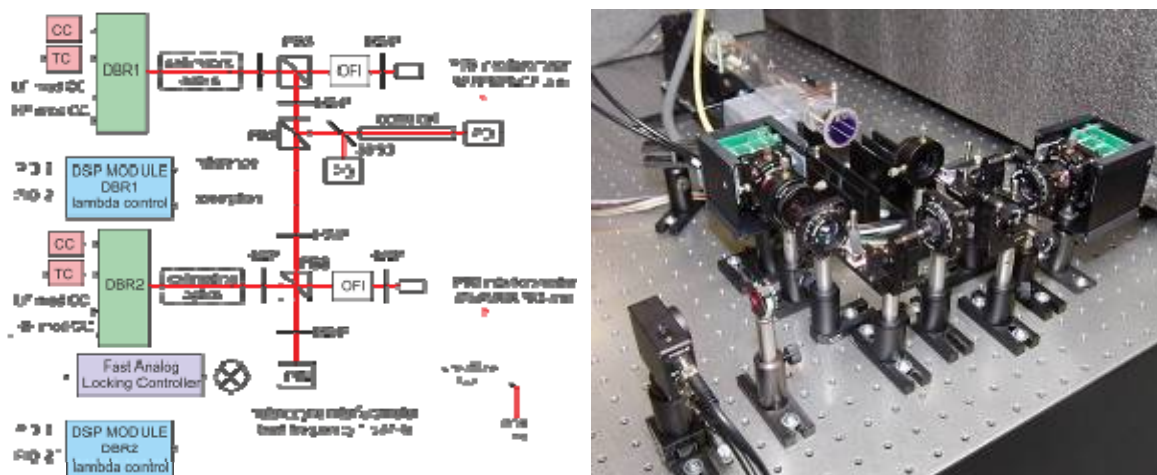


Figure 21: Arrangement of the stabilization setup for a set of two DBR lasers to iodine transition and to constant rf beat frequency and photo of the experimental arrangement.

A special design of a fast analog lock controller (FALC) for the stabilisation of the beat frequency offers high-speed servo control of the laser optical frequency. Recordings show a linewidth of the beat signal of the two DBR lasers under free-running conditions of 3.6 MHz while with the lock on the linewidth has been reduced to 1 Hz (Figure 22).

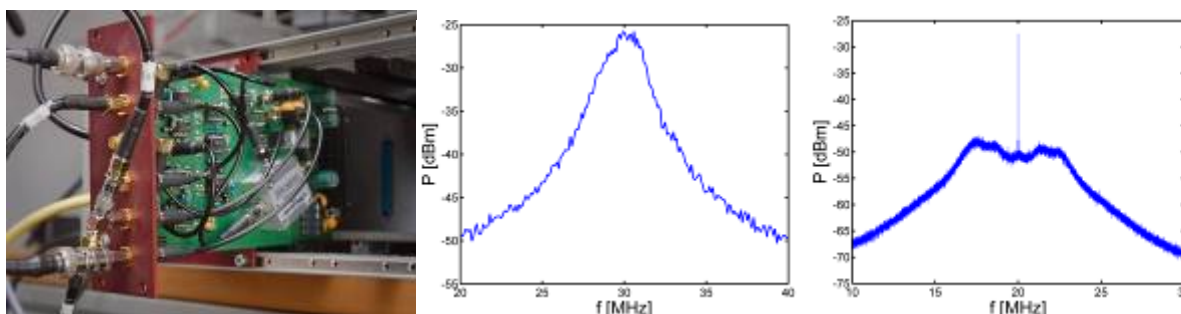
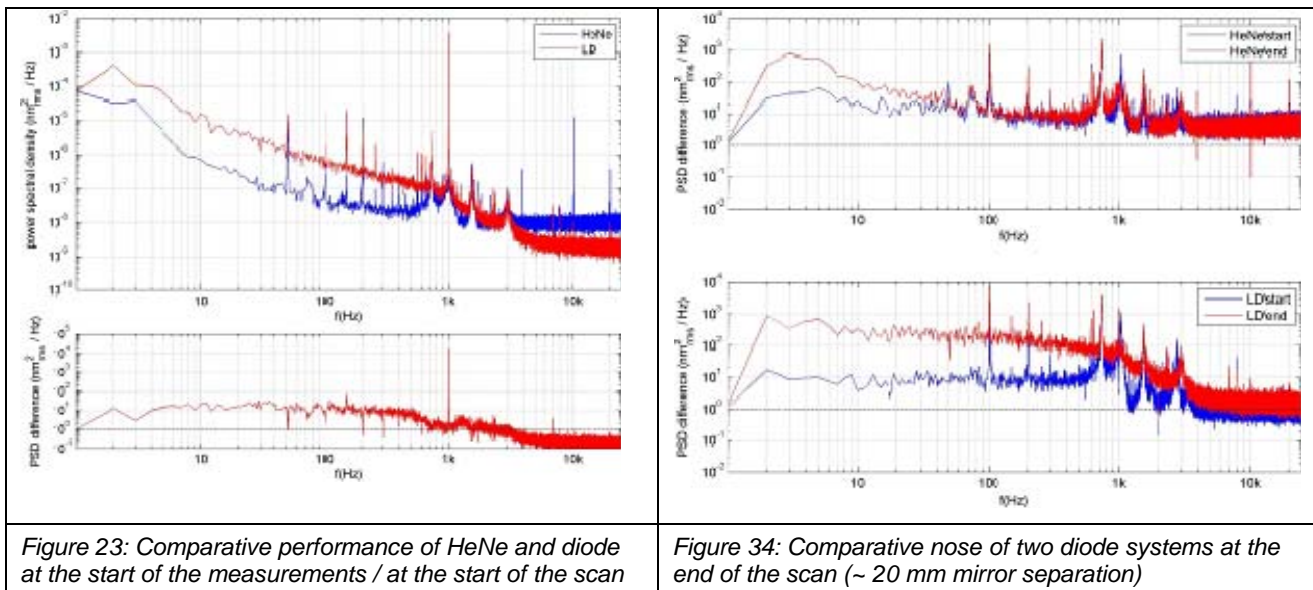


Figure 22: Photo of the FALC controller, free running beat frequency of two DBR lasers and beat frequency under control of FALC.

The results indicate that the DBR diode laser system provides a good laser source for applications in dimensional (nano)metrology since it provides more output power and advanced tunability options than stabilised He-Ne lasers while maintaining fundamental requirements such as the frequency stability, coherence length, noise performance and also a defined traceability.

ISI demonstrated the capability of stabilising a laser diode operating at 633 nm with an iodine cell. NPL worked with ISI to evaluate the system, for use in dimensional metrology applications. An ISI scientist was seconded to NPL and compared the performance of the diode based system with that of a conventional commercially stabilised laser. We set up a system to measure the displacement of a scanning stage with several millimetres range using an NPL Plane Mirror Differential Optical Interferometer that was illuminated in turn with either the laser diode or the HeNe laser. Figure 23 shows the noise spectrum at the start of the scan and figure 24 shows the noise at the end of the scan (~ 20 mm)



The results indicate that the laser diode based system is a suitable alternative for the use in nanometrology in place of the stabilised HeNe laser especially where high output power and also the wide-band mode-hop free wavelength tuning options can bring significant benefits, i.e. in multi-axis displacement metrology or absolute homodyne interferometry. We expect that our future work will lead towards these challenges in which several issues such as improvement of coupling, intensity stability incorporation and achieving a more compact form factor need to be addressed.

Conclusion

A simultaneously measuring 6 axis interferometer was developed. Due to the easy optical design and the large acceptance angle, which could be achieved by using CMOS cameras and an FPGA for the data processing, it allows for a nearly ideal device for checking machine axes and performing acceptance tests on site.

In addition a laser diode based stabilised light source was set-up. It could be demonstrated that the diode could be stabilised to an iodine absorption line. The frequency stability is comparable to a HeNe laser while allowing for a higher output power and a more compact device which is important for a transportable device. The stabilisation technique can also be applied to material length references, which allows for a first order compensation of air refractive index and thermal dilatation of a machine, which makes it a perfect companion for 6DoF interferometer for on site acceptance tests.

This research presents the results for the project objective, 'Development of a compact interferometer to simultaneously measure all six degrees of freedom from one interface' and the target of the research has been met.

3.3 Implementation of methods for the characterisation of motion systems with large angular motion like hexapods or stacked systems with mixed angular and linear motion axes.

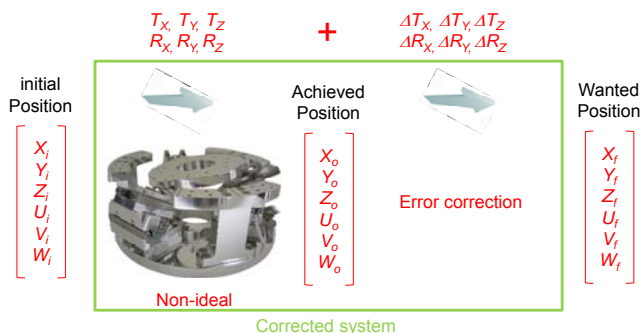
Introduction

With the advent and the affordability of small piezo actuators, hexapods and other multi-axis actuators are more and more commonly used in scientific and industrial applications. Such 6 degrees of freedom (6DoF) systems are for example applied in focussed ion beam (FIB) nanofabrication processes, for sample positioning in particle accelerator beam lines and micro assembly lines. These systems include line scales on all drive axes and often claim nanometre resolution. Nevertheless, their accuracy is often not even mentioned since their geometry is complex and is often based on parallel cinematics. It is thus very difficult to link the motion errors of each axis to the motion error of the output stage. The calibration of such systems is thus not straightforward.

In addition, for a complete calibration, one would like to map the whole actuator working volume. But with 6 degrees of freedom, the number of calibration positions to be measured increases with the power of 6. With for example only 10 calibration positions per axis, mapping the complete volume with such a grid would require measuring 1 million positions! This obviously requires too much time and more efficient calibration methods are required.

Calibration procedure

The calibration procedure for a 6DoF positioning system needs to be smart enough to be independent from the actuators geometry and efficient enough to rely on a small number of measured positions since a complete mapping of the working volume is obviously too time consuming. Therefore a mathematical model for compensation of positioning errors was developed. The general mathematical model proposed here is given in figure 25. It is a polynomial correction applied to a 6 components vector equation. The number of correction parameters increases with the power of the polynomial order if all cross-parameters are considered. For a 2nd order correction this represents already 156 parameters. A complete 3rd order correction would require 912 parameters. In general, not all parameters are required so one can hope to obtain a good correction using only a few selected correction parameters.



where the 6 terms of the error correction are given by:

$$\Delta_i = C_i + \sum_j C_{ij} j + \sum_{jk} C_{ijk} jk + \sum_{jkl} C_{ijkl} jkl + \dots$$

with $i, j, k, l, \dots = T_x, T_y, T_z, R_x, R_y, R_z$

Figure 25: Mathematical model for the error correction. The model is similar to a polynomial correction but applied to a 6 component vectorial equation. The number of parameters increases with the power of the polynomial order used.

Measurement strategy

Choosing the optimal positions to measure within the working volume was done according to the following considerations:

- 1) Measuring positions along each main axis of the 6DoF Cartesian coordinate system, leaving the other axis centered, should already give a good hint about the correction. Cross terms should be less important. In addition, for 6DoF systems like hexapods, the travel range along the main axes is usually longer than with combined axes motion. Therefore a rather high position density along the main Cartesian axes was chosen.
- 2) Mapping all positions on a grid in the 6D volume quickly generates a lot of positions, thus a lower position density was chosen which covers the largest range of reachable positions within the working volume. In addition, one may want to keep some symmetry for applying error separation techniques. A volume mapping over a minimum 3x3x3x3x3x3 grid for a 2nd order correction already represents a total of 729 positions to measure.

Calibrations

The calibration procedure has been applied to the 6 DoF piezo stage shown in figure 26. The system has a full range of ±10 mm in X and Y, ±5 mm in Z, ±10 ° in Rx and Ry and ±17 ° in Rz, but its reach is limited to about 1/3 of the range for combined axes motions. This 6DoF positioning system is small enough to be placed on the METAS μ-CMM. The system can thus be accurately calibrated by probing at each position 3 of the spheres attached on its output stage.

Following the previously mentioned strategy, positions every millimetre and respectively ever degree along the main axes and positions at 1/3 of the axis ranges on a 3x3x3x3x3x3 grid in the



volume were measured. It took almost 2 days to measure all the 867 actuator positions.

The positioning errors of the 6DoF system are given in figure 27, plotted vs the position number. The first positions were measured along the main axes followed by the systematic mapping of its working volume at a 3x3x3x3x3x3 grid. One can observe that the positioning errors shown on the figure 27 follow a certain systematic pattern. This pattern was used to identify which correction terms are strongly needed and which can be neglected. For instance, the errors along the main axes are mainly corrected with the linear and some of the quadratic components. The cubic terms can be neglected. A simple solver was used to find the optimum values of the correction parameters using the least square of the 3D position errors given by the equation in figure 25. Figure 28 shows the positioning errors after optimizing all offset, linear and 18 quadratic correction terms. Finally figure 29 shows that even smaller deviations can be reached by adding only 4 more specific cubic correction terms to the correction model. Corrected positions deviations remain mostly below 2 μm and 0.005 $^\circ$ which is a good result knowing that the positioning repeatability of the hexapod is about $\pm 0.3 \mu\text{m}$ and $\pm 0.15^\circ$.

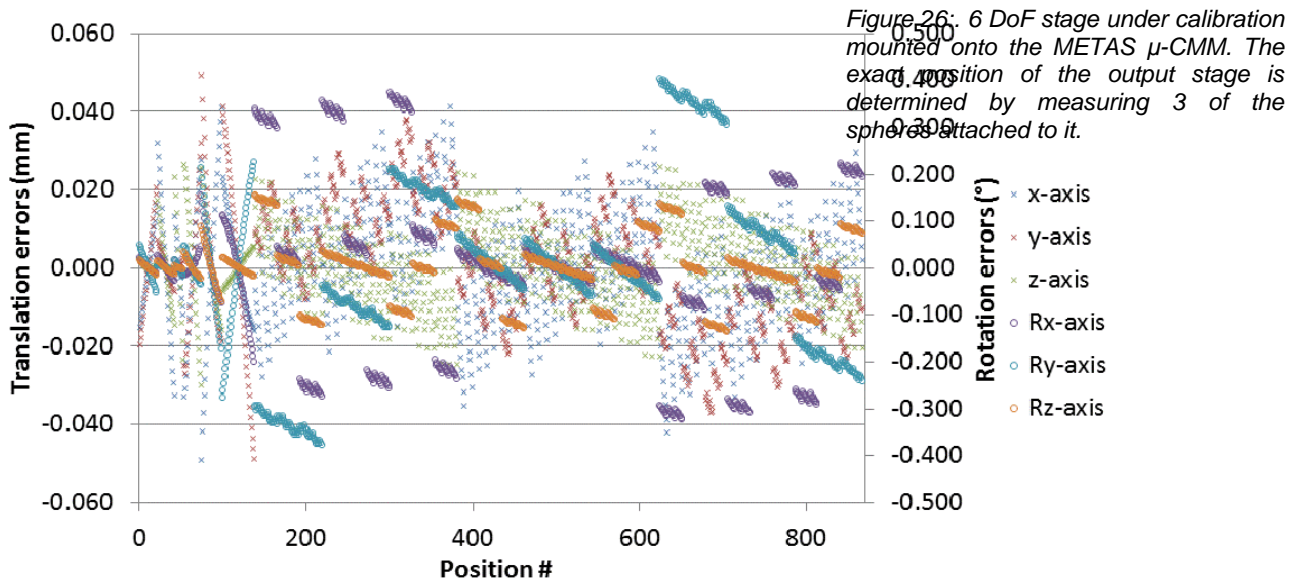


Figure 27: The positioning errors without any correction go up to $\pm 50 \mu\text{m}$ and $\pm 0.4^\circ$.

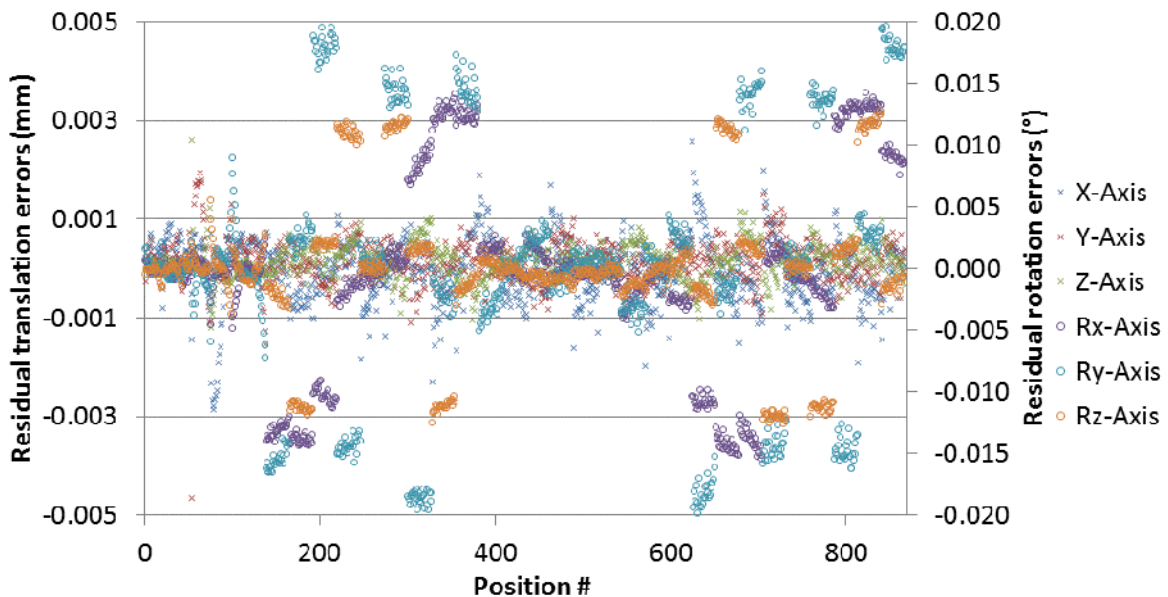


Figure 28: The positioning errors after optimizing all offset, all linear and 18 quadratic correction terms. Errors are corrected down to $\pm 5 \mu\text{m}$ and $\pm 0.02^\circ$, but the introduction of some cubic correction terms is needed.

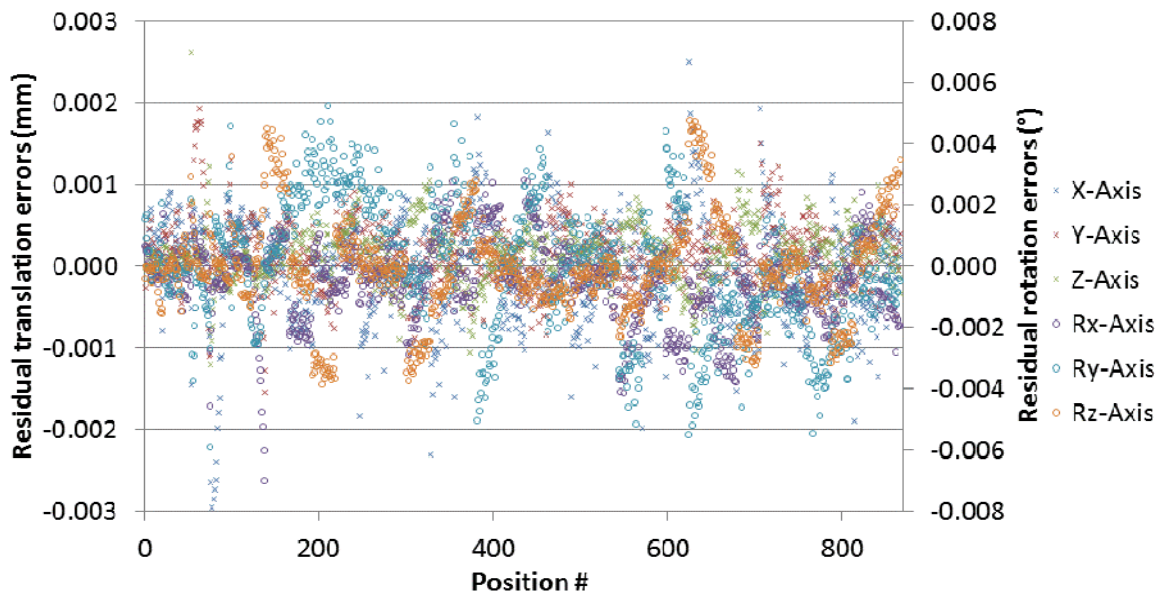


Figure 29: The positioning errors after optimizing all offset, all linear, 18 quadratic correction terms and 4 cubic terms. Errors are now corrected down to $\pm 3 \mu\text{m}$ and $\pm 0.007^\circ$.

Physik Instrumente, as a stakeholder, kindly lent METAS and PTB one of their Hexapod, model H-840.D2, for testing and calibration. METAS applied the identical calibration method as described previously, but due to the much larger size of the hexapod, using its SIP Orion CMM. The measured positioning errors without correction were below $50 \mu\text{m}$ and 0.02° . After calibration, the positioning errors were reduced to $5 \mu\text{m}$ and 0.002° within the whole calibrated volume.

Lasertracer based 6DoF Measurements on Hexapod (PTB)

One of the goals of the project was to verify the positioning capabilities of the hexapod PI H-840 using two different methods. For the comparison to tactile measurements obtained by measurement on a CMM performed by METAS, the positioning accuracy was checked using the M3D3 multi-lateration technique at PTB. For this purpose, a set of four tracking laser interferometers, i.e. Laser Tracers, and the hexapod under investigation were set up on a sturdy granite plate. The laser tracers and the hexapod were arranged as shown in Figure 30. All four laser beams were aligned to hit a 2-cm-sized cat eye reflector attached to the top plate of the hexapod. The laser tracers automatically tracked the ball-shaped reflector and continuously measured the distances to the reflector. Based on the principle of multilateration 3D point coordinates (x, y, and z) were calculated using the measured length changes.

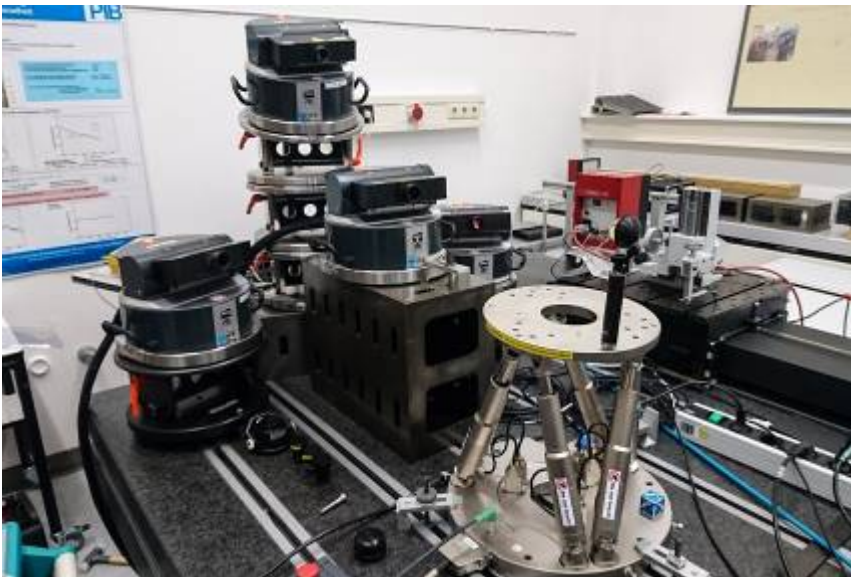


Figure 30: The image shows the hexapod setup used at PTB to determine the positioning accuracy of the device. The cat eye reflector was placed at three different positions on top of the hexapod

To obtain a dataset for comparison to the conventional tactile measurements, the same position commands as used on the CMM were executed and after reaching the target position the current position was recorded using the laser tracers. All positions were measured multiple times. For separating different error sources (i.e. all six degrees of freedom) the reflector was placed at three different positions on top of the hexapod, separated by 60 degrees each, and at two different heights above the top plate. The sequential measurement of the three setups requires a good reproducibility of the Hexapod poses and moreover the stability of the Hexapod and Laser Tracer positions throughout the whole

measurement procedure compared to the CMM calibrations performed at METAS, where the three points can be measured after one pose of the Hexapod, where only the position stability matters and not the positioning repeatability. Additionally, the time between the measurements of the three ball positions is shorter in comparison reducing the stability requirements of the measurement setup. Therefore, it was essential to keep the overall measurement time as short as possible. That is the reason why we decided to implement a special software which controls the experiment and is based on our multilateration toolkit.

When examining the data it became apparent that the data reveal discrepancies, which prevent a full analysis of the geometric errors of the hexapod. Figure 31 illustrates the problems that occurred during the measurements. Each measurement setup consists of ~3000 Hexapod poses controlled by our measurement software. At each pose the software should wait for the standstill signal from the Hexapod controller and afterward read out ~10 times the distances of all four Laser Tracers and all Hexapod axes. The standard deviations of the readings at one position during the expected standstill are a measure for the quality of the measurement. For the distances measured by the laser interferometers the standard deviations were mainly in the sub micrometre range (see diagrams in **Error! Reference source not found.**). However, at certain positions we recorded standard deviations in the millimetre range. This can happen if the Hexapod was still moving or if unrecognised beam breaks have occurred. Another effect in the millimetre range can be seen in reported Hexapod positions, coming probably from communication problems with the Hexapod controller. Unfortunately, both effects are not synchronised, which suggests various causes. Anyway, poses showing at least one of these effects have not been part of the multilateration procedure. In the end, we had to reject roughly the half of the originally measured points.

For a first overview, we compared the fitted reflector positions considering only poses without rotations. They should fit together very well, except that they are shifted by offset of the retro reflector. **Error! Reference source not found.** reveals an unexpected high systematic deformation of the measure point pattern which can be caused by the above-mentioned error sources. When looking only at the residual errors, which are in the sub micrometre range, it could be shown that the multi lateration measurements are consistent and suitable to characterise Hexapod systems.

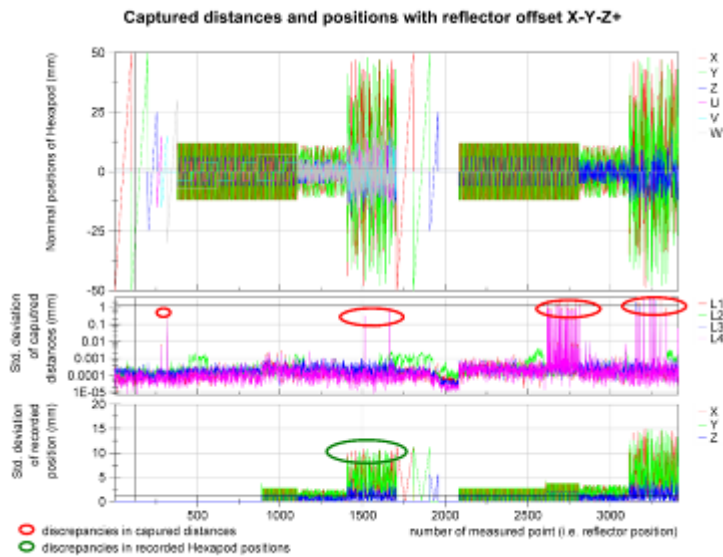


Figure 31: Diagrams of captured distances and Hexapod positions to illustrate problems during measurements

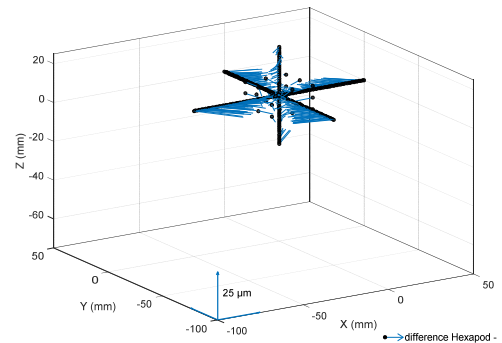


Figure 32: Spatial differences between fitted reflector positions and Hexapod position (no nominal rotations)

Conclusion

METAS now possesses a procedure for calibrating 6DoF systems where no pre-knowledge of the actuator geometry is required and the procedure is general enough to be applied to any 6 DoF actuator geometry. As demonstrators, a piezo motor driven 6 DoF actuator small enough to fit into the measuring volume of the METAS μ -CMM and a big Hexapod were used. The implemented correction shows in the two cases an improvement of the positioning accuracy of 20x in translation and 50x in rotation for the small 6DoF piezo driven stage, and of 10x for the big Hexapod.

Laser tracer measurements are also suitable to perform Hexapod calibrations in the sub- μ m range and an optimised data processing for such calibrations were developed. As for simultaneous measurements too many tracers are necessary to provide an economical solution and measuring the path of the Hexapod sequentially with the tracking mirror at different positions generates higher measurement uncertainties than measuring three balls sequentially at the same position in a CMM. Laser tracers are especially suited for large scale Hexapods.

This research presents the results for the project objective, 'Implementation of methods for the characterisation of motion systems with large angular motion like hexapods or stacked systems with mixed angular and linear motion axes' and the target of the research has been met.

3.4 Calibration and error mapping in six degrees of freedom of nanopositioning stages regarding positioning errors, angular deviations, straightness of motion and orthogonality.

Introduction

The recent growth in availability of nanopositioning devices together with the demand for improved positioning accuracy is driven by the increased need for nanopositioning in a variety of sectors throughout academia and industry ranging from microscopy to space science. Although commercially available stages have high resolution, manufacturers often supply no information about the errors associated with the stage and there is no common format for presentation of stage performance. Many NMI applications require not only precise but also accurate nanopositioning with traceability and measurement of stage performance that includes an uncertainty analysis. To achieve this a test bed was proposed, designed and constructed to evaluate nanopositioning stages. It was initially planned to use a fibre optic based interferometer that would have been developed within the project, but after problems associated with the development of the interferometer, bulk optics were used instead.

Testbed and laser interferometry

The Testbed (Figure 33) comprises three orthogonal NPL Plane Mirror Differential Optical Interferometers and two orthogonal two axis autocollimators, constructed at CMI, that measure stage angular errors. The orthogonality of the test bed is given by a high precision glass cube mirror used as a reference surface. The orthogonality of the cube faces is better than one arc second.

Work started on the development of a fibre interferometer for displacement measurement. The aim was to use this in the stage testbed and for characterizing the HSAM scanning stages. Initial work concentrated on a homodyne system based on achieving quadrature using different polarisations of light in the interferometer. This was based on work previously reported by Pullteap and Seat (S Pullteap and HC Seat, "Investigation and compensation of polarization-induced signal fading in an extrinsic fibre-based Fabry–Perot interferometric vibrometer," in IEEE/ASME International Conference on Mechatronics and Embedded Systems and Applications (IEEE, 2012), pp. 12–17.).

We found that there were severe instabilities in the fibre due to birefringence and that we could not achieve continuous stability and therefore were unable to maintain a continuous quadrature relationship between the two output signals. While it was possible to mitigate against this in a dynamic system, it was not suitable for our purposes where drift measurements in a quasi-static system were also required. Consequently we decided to concentrate on a bulk optics approach and use conventional bulk optics for the interferometers. However, discussions with ISI early on in the project identified the possibility for further work investigating the suitability of laser diodes as an alternative to a helium neon laser so effort was directed towards this goal.

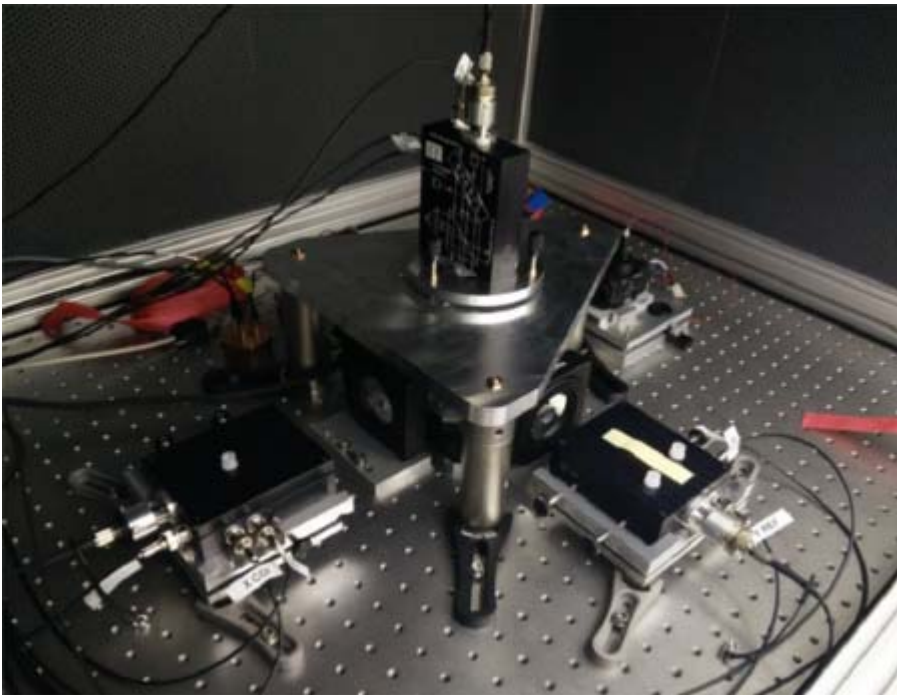


Figure 34: showing the Test bed for stage characterisation

Software was written by NPL for data collection; interferometer position, autocollimator readings, stage target position and position as measured by the stage's internal sensors. Processing of the data was done offline using routines that were written by CMI. An uncertainty budget was jointly prepared by NPL and CMI. Several stages have been examined and errors mapped. The data are stored as GWYDDION files (<http://gwyddion.net>), a separate file is created for every measurement at constant height (for xyz stages the individual z values are measured separately). Using GWYDDION software we load all the measured data,

including repeated measurements and we process them using a dedicated standalone module within GWYDDION. The following data processing is done:

- Interferometer data is Edlen corrected to mitigate environmental changes causing refractive index variations leading to errors in the dead path
- Differences between interferometer and stage sensors are evaluated
- Differences are averaged if multiple measurements were made
- (Averaged) differences are rotated to minimum deviation between stage and test bed axis
- (Averaged) rotations are evaluated from autocollimator channels.

- Uncertainties are evaluated: if multiple data for the same height are provided the A uncertainty is evaluated from them. B type uncertainty is evaluated from local rotations (for Abbe error) and other fixed terms that are obtained from analysis outside of GWYDDION.

As a result, the stage errors (averaged and rotated differences between stage sensors and test bed), rotations, and a lookup table for correction of the stage position are provided.

The output data show the difference between the stage target position and the actual position as measured by the interferometers. An example of the output data is shown in figure 34.

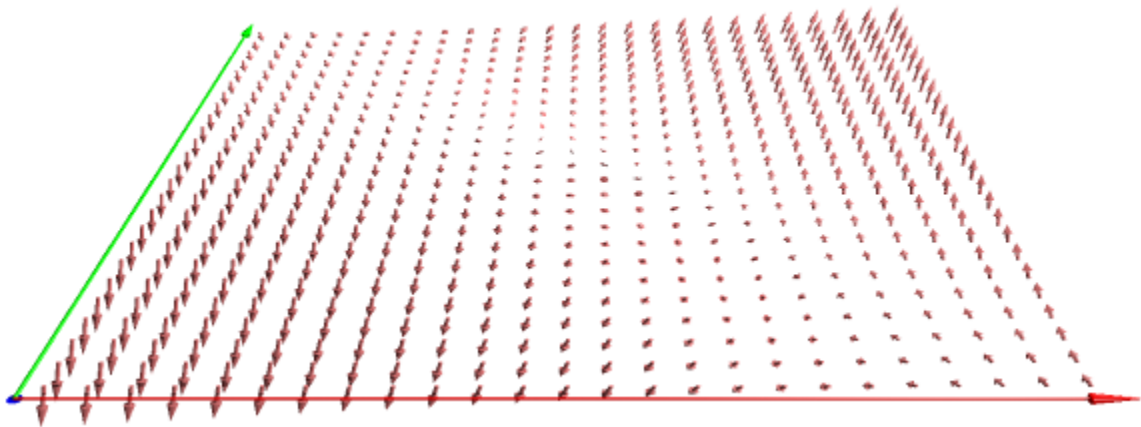


Figure 34: stage positioning errors result obtained from 5 repeated scans over 100x100 micrometres. The length of errors shown as arrows is multiplied by factor of 10.

Towards the end of the project, the collaboration between CMI and NPL led to ideas for *insitu* methods for stage error evaluation. These will be pursued after the end of the project and verified using the Test Bed.

Atomic flat surfaces

Lateral parasitic motion of nano-positioning stages can introduce flatness measurement errors. Over the short stroke of the stages straightness errors due to topography errors of the mirrors are strongly suppressed by the comparable large diameter of the interferometer beam. A check for the remaining errors can be done by a perfect flat surface, which was manufactured on silicon by PTB. The technology is based on temperature treatment of the surface in a ultra-high vacuum. The surface borders are determined by lithographically generated borders. The flat areas can be manufactured up to 200 μm square as shown in figure 35. The surface gets under atmospheric environments a homogenous oxide layer with high stability.

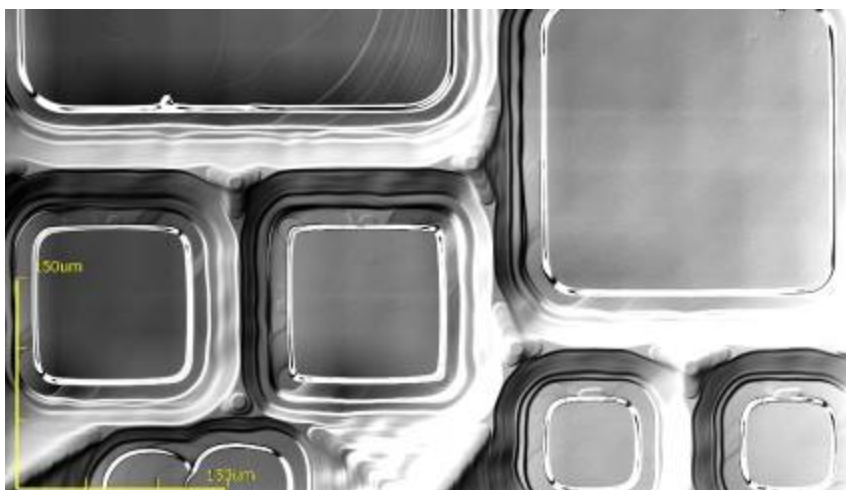


Figure 35: Atomic flat silicon surfaces.

Metrology high speed AFM

Throughout the project NPL, CMI and University of Bristol worked together with the aim of characterising scanning stages used for high speed AFM. Some initial work was done on the test bed, but generally the test bed is designed for lower speed stages. Later it was decided to establish a metrological high speed AFM facility at NPL and to have dedicated interferometers for the set up. The scanning system is shown in figures 36 and 37. This can also be used for stage characterisation.

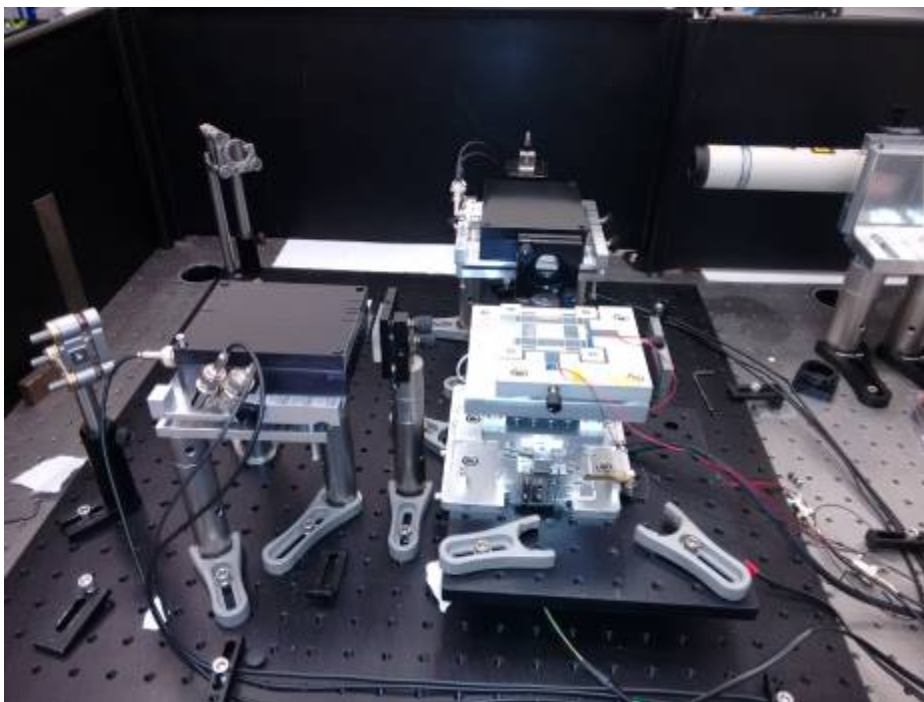


Figure 36: showing the scanning platform for the HSAFM facility being developed at NPL

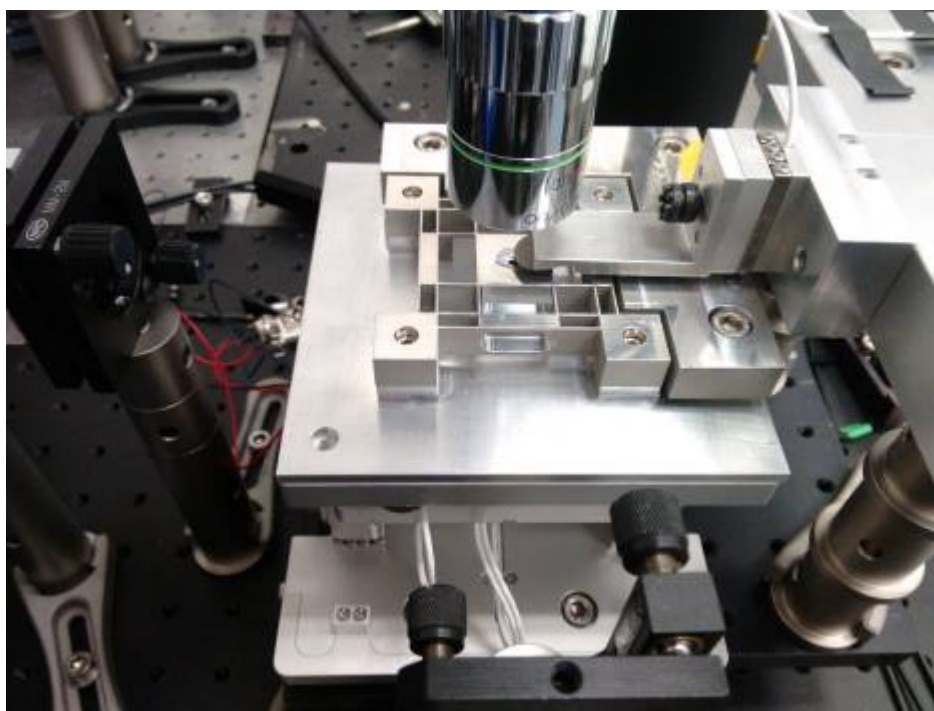


Figure 37: shows a close up of laser Doppler Vibrometer used to detect AFM cantilever motion.

These scanning platforms were used to characterise a larger than normal high speed stage. The stage had a scan range of $4\ \mu\text{m} \times 4\ \mu\text{m}$, was scanned a 1 kHz in the fast axis and 1 kHz in the slow axis thereby acquiring 4 frames per second. The results identified cross talk in the stage between the two axes, non-symmetric motion on trace and retrace scans and a phase offset between the drive signal and the motion of the PZT. All of these terms led to errors in the High speed AFM system and we have shown that we can mitigate for them. An example of this for a preliminary set of data is shown in figure 38.

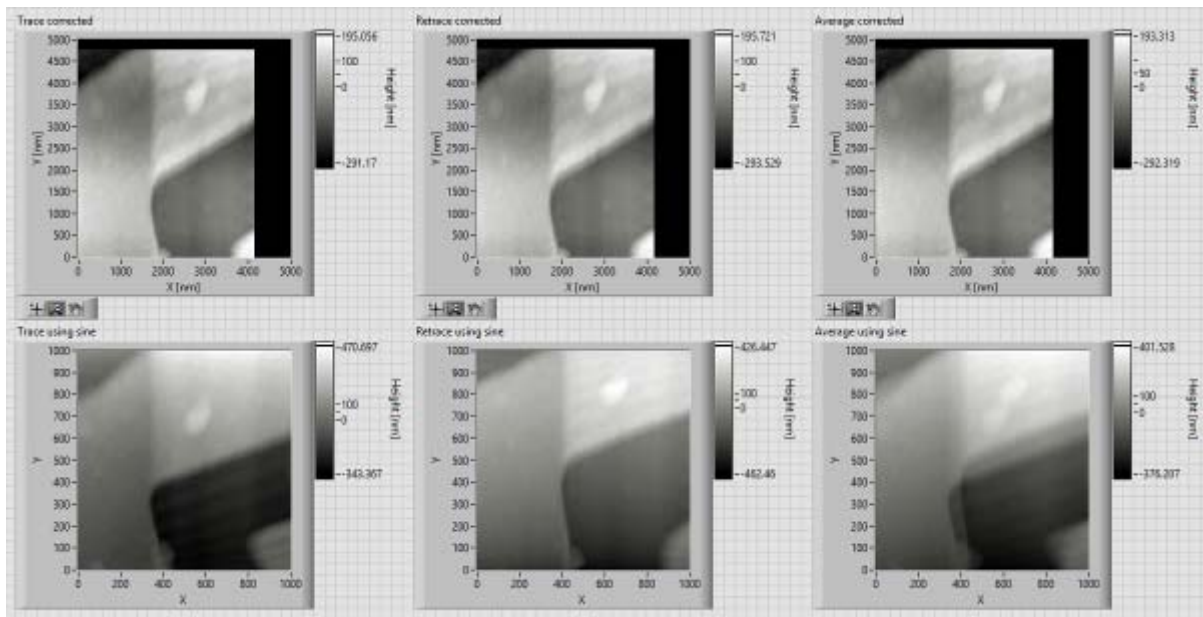


Figure 38: shows high speed AFM data. Top line shows images based on interferometer data, bottom line shows images based on pzt drive signal data

The top line shows images based on the optical interferometer signals and the bottom line shows images based on the voltage supplied to the PZT. In both cases the left hand image is the trace image (forward scan) and the right hand image the re-trace image (backwards scan). The right hand image is the superposition of the trace and retrace images. The interferometer based images is much sharper and compensates for the errors in the scanning stage. Development of this technique will allow NPL and Bristol University to establish traceability for the technique and turn it from a qualitative imaging technique into a quantitative technique with a known measurement uncertainty.

Conclusion

A testbed for the calibration of nano positioning devices was built. Exemplarily a stage of a high speed AFM was characterised and a large improvement in linearisation of the generated images could be shown. The interferometry of the testbed was integrated in a new scanner to set-up the World's first metrology high speed AFM. The testbed allows NPL to supply a new calibration service for stage manufacturers and AFM users.

This research presents the results for the project objective, 'Calibration and error mapping in six degrees of freedom of nanopositioning stages regarding positioning errors, angular deviations, straightness of motion and orthogonality' and the target of the research has been met.

3.5 Improvement of the measurement speed of AFM to allow measurements of larger areas and to reduce drift in the instrumentation.

Introduction

Scanning probe microscopes and similar techniques that are based on evaluation of some local interaction between a sensing element and a sample surface are very often limited by the scanning speed. The reason might be time scale of the interaction itself or need for preserving geometry of a fragile probe. In metrology instruments there is also need for evaluating multiple detectors at each individual position of the probe or

performing some averaging. All these effects increase the time necessary for the measurement which not only limits the measuring technique throughput, but also increases influence of thermal or mechanical drifts on the measurement.

Long range AFM measurements are afflicted with the drift due to the long measurement times and from the tip wear due to the large measured distances. The goal of this work is minimising drift, tip wear and therefore the measurement uncertainties in long range AFMs. This research deals with the investigation and improvement of the long term stability of the AFMs, as well as with the practical determination of the tip wear during the scan plus with the different enhanced scanning strategies.

For large range AFM the measurement uncertainty is strongly influenced by the specific measurement tasks e.g. due to larger guidance errors, larger drift caused by longer measurement times. A virtual AFM which uses Monte Carlo methods can be used to determine the specific uncertainty for measurement tasks and practical implementations of the measurement sequence. This way the virtual AFM can be used to optimize AFM scanning paths.

Scanning Strategy and Software

In order to speed up the measurements CMI and NPL have developed a set of algorithms for non-equidistant scanning support in scanning probe microscopy techniques. Non-equidistant (adaptive) scanning is a novel approach for reducing the time necessary for measurement by measuring only the data that will be used for evaluation in the data processing phase. While the principal idea is very simple, there are many obstacles if someone wants to implement it on a measuring instrument. Regular data placed on an equally spaced grid are easy to preview and can be processed in many data processing software tools. In contrary, there is almost no support for more general surface data that are not equally spaced and it is therefore complicated to even preview such data. The library developed with in this project, together with data processing functions implemented in GWYDDION open source software will make the use of non-equidistant data much easier.

The Gwyscan library is written in C and is independent of any other data processing software in order to make it easily embeddable in various devices. So even though data are stored in GWYDDION-compatible formats, it is not necessary to have GWYDDION installed on the computer where the microscope is operated. The library defines basic data structures and provides the following three sets of functions:

- scan path generation,
- preview of the data via interpolation onto regular grid, and
- storage of data in GWYDDION-compatible, publicly available formats.

As many of the custom built SPMs are operated using the LabVIEW environment from National Instruments, we have also implemented a LabVIEW interface to the library. The conversion between the two languages involves a handling of pointers which has been managed to ensure an efficient flow of data and memory storage and should be invisible to the LabVIEW user. In principle, to use the routines with a homemade AFM one needs to have the drivers for the scanning stage being used; these are most commonly supplied in a LabVIEW format, and then it is relatively simple to implement the library routines. This was demonstrated during the developmental work, when the GWYDDION routines were implemented into a client program at National Physical Laboratory in London (UK) that allowed remote operation of the AFM at Czech Metrology Institute in Brno (Czech Republic) over a distance of 1200 km.

The **scan path** is simply a set of (x, y) positions that the SPM probe should follow. The user can setup the scanning path in an arbitrary way and the measured data can be still further processed using the other algorithms presented in this paper, however the library already includes some pre-defined scanning paths with different statistical properties. There are two main classes of scan paths: single scan paths forming an entire image at once and refinement paths helping to add some more detailed measurements to previously measured data. Some of the basic scanning implemented in the library paths are shown in figure 39. They differ in their statistical properties, especially isotropy and are suitable for different tasks.

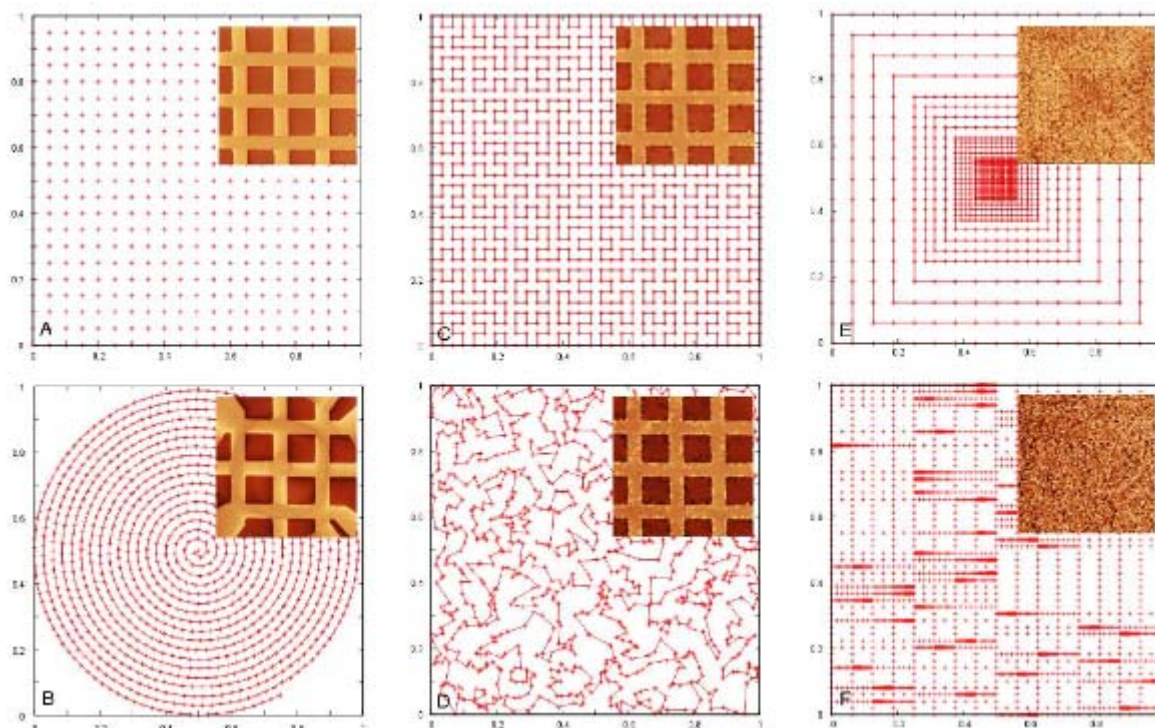


Figure 39: single scanning paths: a coarse path visualization and a real measurement (inset): (A) regular scan path, (B) spiral scan path, (C) space filling scan path, (D) random scan path, (E) 2D octave scan path, (F) 1D octave scan path. Calibration grating is displayed for paths A–D, random roughness on silicon on paths E–F.

The most frequent operation that we need to perform with the data is a **preview**, typically used while scanning to obtain quasi-real-time information. A simple preview function is part of the Gwyscan library so it can be used to feed the SPM graphical user interface with raster data compatible with what would be obtained via regular scanning approach. As triangulation is unnecessary and can be too computationally demanding for this purpose, a fast algorithm that works as follows is used instead:

- (i) A regular grid is set up, matching the scan area and desired pixel resolutions.
- (ii) For a pixel in which some data have been measured a weighted average of data falling into this pixel is computed.
- (iii) The remaining pixels (with no data) are interpolated using a value propagation from pixels that have already a value assigned, similarly to the flood-fill algorithm.

The preview image therefore approximately corresponds to binning in areas where a large number of measurements lie in one pixel, and to nearest-neighbor interpolation based on Voronoi tessellation in regions where measurements are sparse.

Finally, data are **stored** and further **processed** in GWYDDION (<http://gwyddion.net>). This includes data triangulation onto a regular grid, as most of the data analysis tools used in SPMs still assume that data are regularly sampled. Here, user can select, based on local data density, the appropriate resolution and range of the data that should be regularised. It must be noted that this is a data extraction operation, the non-equidistant data are kept intact and can be processed differently later. In future we also intend to add more data analysis routines working directly with the non-equidistant data.

The benefit of many of the scan paths is that the probe is repeatedly measuring in adjacent parts of the surface with large time delay between individual measurements. At first sight this would be a problem as the drifts in the measuring system might significantly distort the measurement; we have however used this to establish a drift detection and compensation mechanism; within the measurement the drift is automatically estimated and data are corrected. An example of the drift compensation is shown in figure 40.

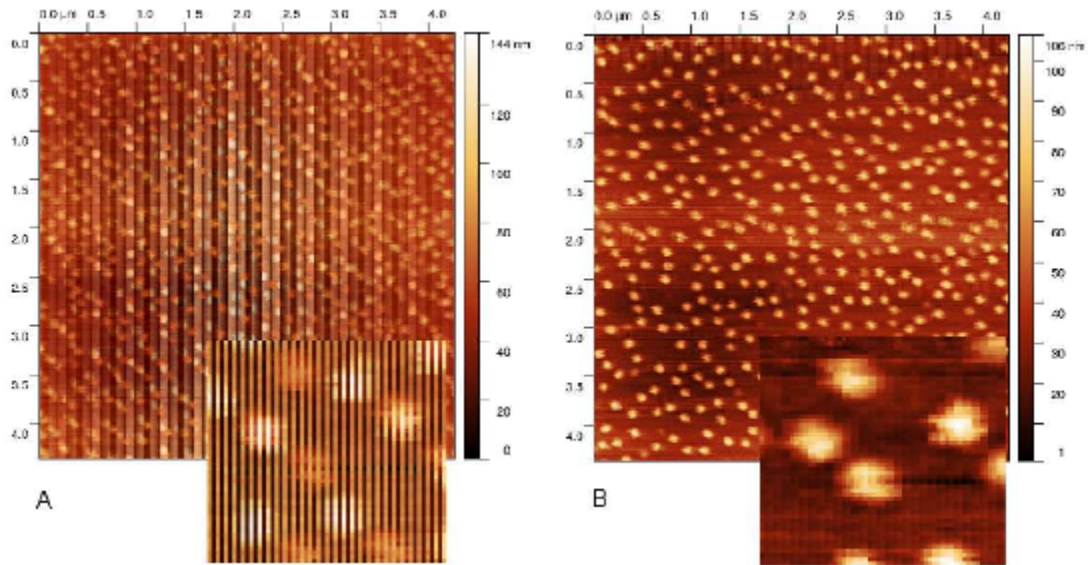


Figure 40: quantum dot sample (by PTB) regularized data (A) prior and (B) after drift correction procedure (an image detail shown in the inset).

As an example of the applications of the library we present an image of the structure measured on a Nanovea test sample together with refinement path and refined data (Figure 41). These measurements were done on a very simple custom built SPM in order to show suitability of the library for systems built from scratch, however any SPM that can be operated on user selected path is suitable for use of the library functions as well.

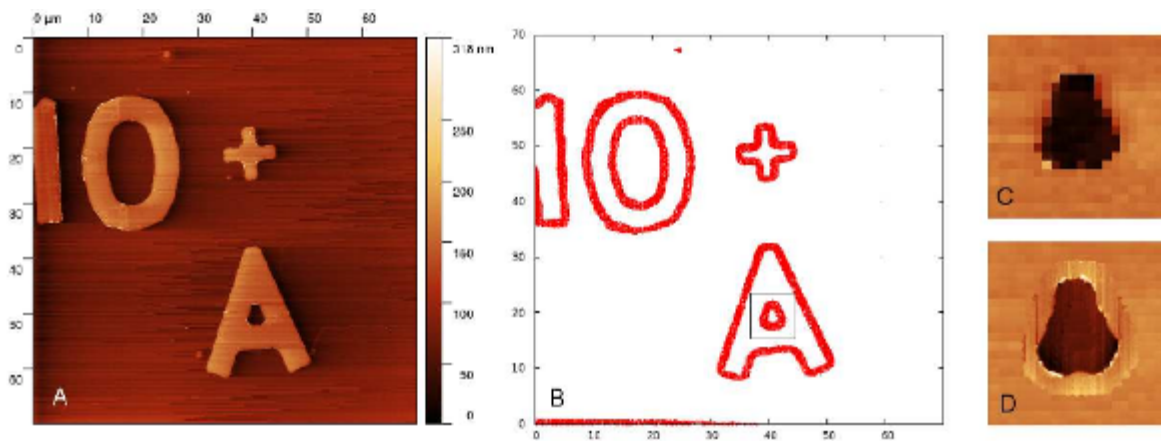


Figure 41: path refinement measurement example: (A) coarse path, (B) suggested refinement, (C) detail of the coarse image, (D) detail of the refined image. The detail location is shown on figure (B).

Different scanning modes have been implemented on the large range AFM at TUIL as described below. The scanning modes can be adapted to the structures to be measured. For round structures a circular scanning reduces the measurement times by a factor of 1.5. The measurements shown in figure 42 given at different lines across the sample gave very similar noise levels for all scanning modes.

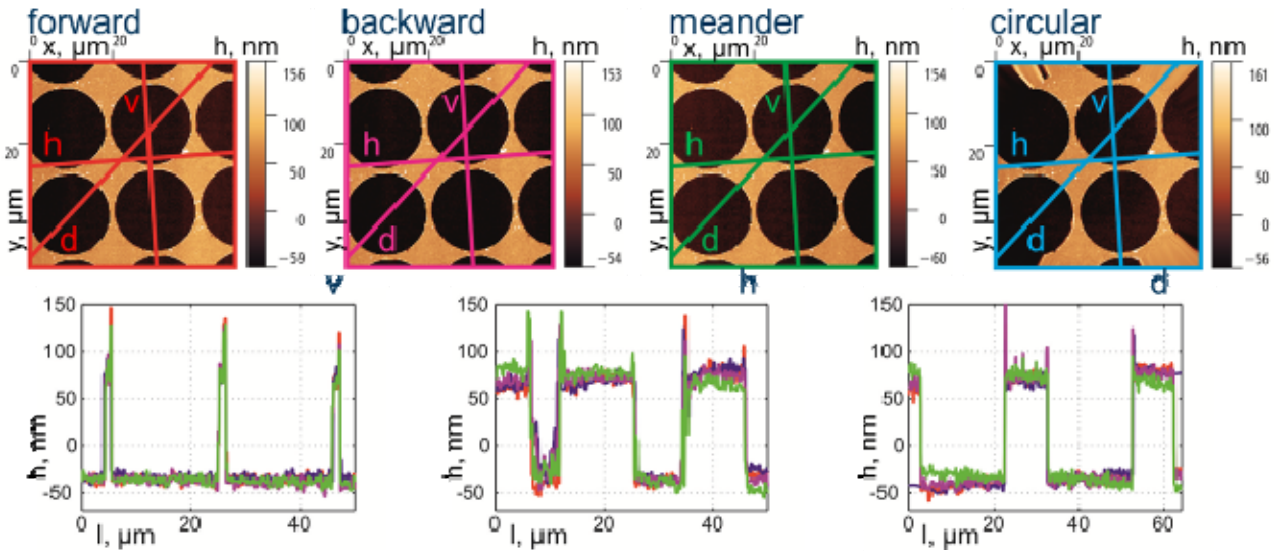


Figure 42: Measurement results on the Nanomeasuring Machine using different scanning paths

On the same AFM a method for an adaptive definition of measurement tasks has been implemented using images from the Camera build in the AFM. An overview was generated by stitching single camera images. The pixels are transformed to the machine coordinate system. The Overview image can be processed by a segmentation and labelling routine originally developed for satellite images. Using these techniques the scan range of the AFM can be minimised by the generated pre knowledge. The procedure is visualised in figure 43.

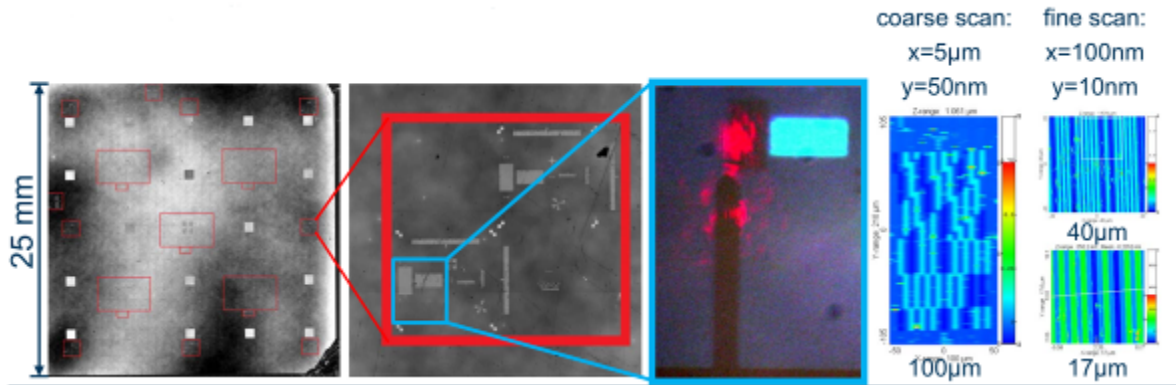


Figure 43: Adaptive Scanning on the Nanomeasuring Machine

Long range AFM

For the investigations of long range AFM the first generation of the Nanometer Positioning and Measurement System (NPMM) of TUIL was used. This system was equipped with a self-developed interferometric AFM head as shown in Figure 44 together with the integration in the NPMM.

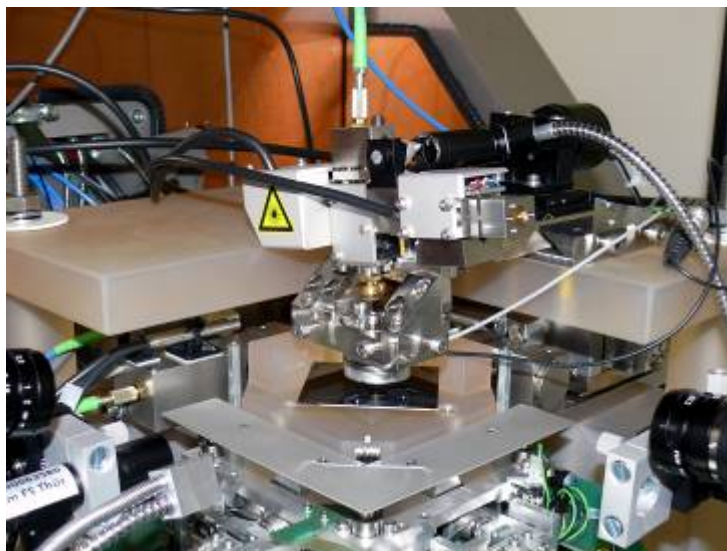
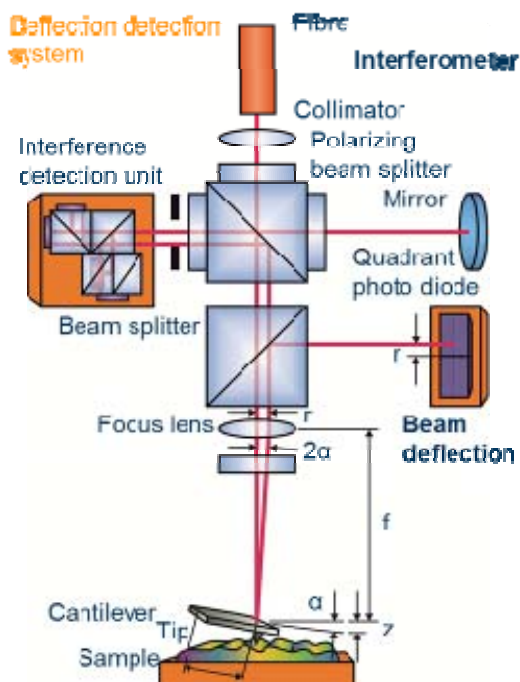


Figure 44: Principle of the interferometer based AFM head of TUIL and the integration in the NPMM

Investigation of the drift behaviour was based on continuous recording of the signals of the AFM head. Particularly important are deflection (bending or oscillation amplitude) and position value of the cantilever. Drift of the deflection signal induce to the changes in the probing forces as well as of the position signal cause to the changes in the height information during the scan. For the practical measurements the information about the waiting time after cantilever replacement and switch-on of the temperature control plus the knowledge about the long term stability of the cantilever deflection and position are especially crucial.

The finite size of the AFM tip and the changes in its shape due to the wear during the scan induce lowering of the lateral resolution and accuracy of the AFM measurements (Figure 45). Because each measured image of the sample surface corresponds to the convolution of the cantilever tip with the real surface. It is important to know the shape of the tip and its wear behavior according to the measured distance and different operational, scanning and surface parameters. The scanning of the TGT1 array of sharp tips and subsequent tip reconstruction is from the practical perspective especial suitable possibility to determine the shape of the AFM tip with regards to long distance measurements.

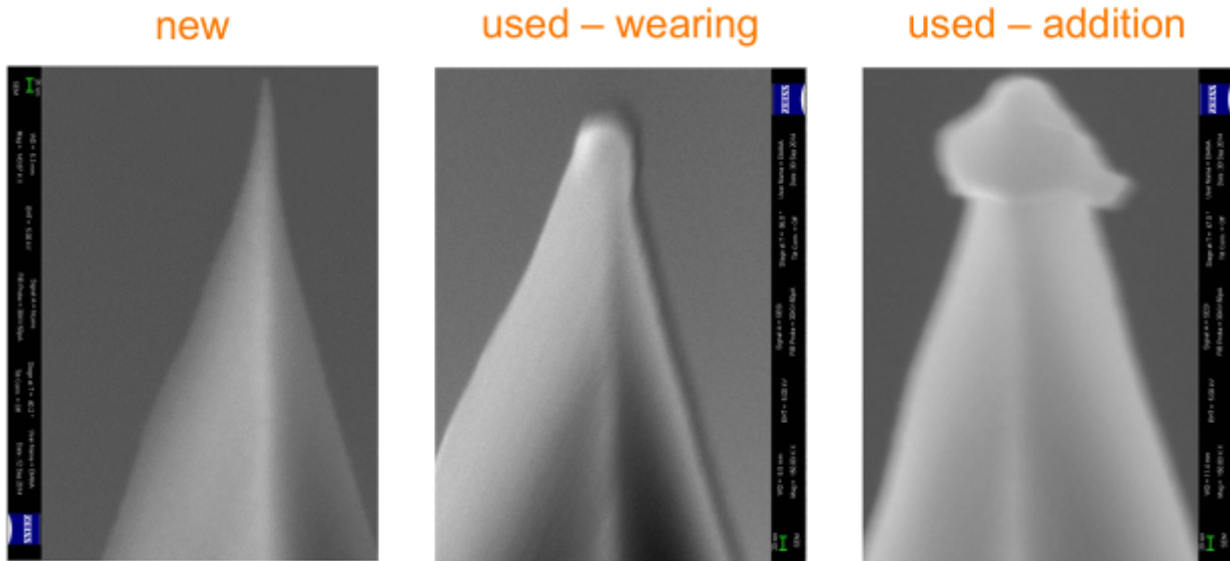


Figure 45: Tip wear visualised by electron microscopy (SEM) images

The experimental wear investigation was based on the successively scan of the tip characteriser TGT1 and the measurement sample. Thereby the intervals for tip characterisation were experimentally decided. The changes of tip form and tip radius serve as the rate of the wear. In this work effect of the scanning speed, probing forces, mode of operation as well as the design of the tip itself on its wear were investigated. 11 different commercially available tips have been chosen. The measuring plan consists on using the tip characteriser first and then generating wear by scanning on a flat surface. The tip characteriser measurements were repeated after 5, 10, 50, 100, 250, 500 and 1000 mm scanning paths.

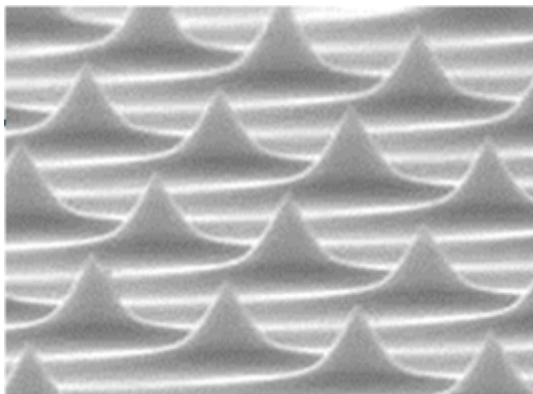


Figure 46: TGT1 tip characterizer

An example for one cantilever is shown in figure 47. Based on all of these measurements a best practice guide for lowering tip wear in AFM measurements was compiled.

- Radius: data sheet 10nm
measured 45nm
- Amplitude: 10nA
- setpoint: 7nA
- $v=20 \mu\text{m/s}$

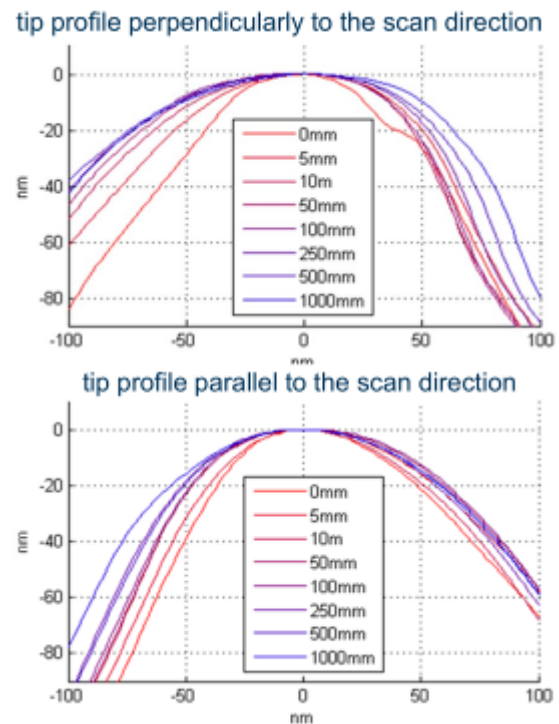
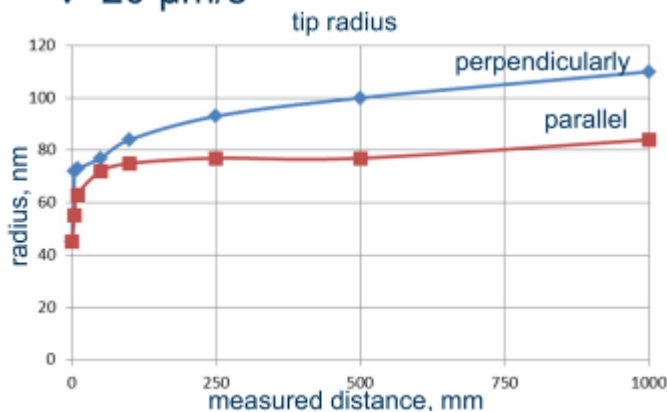
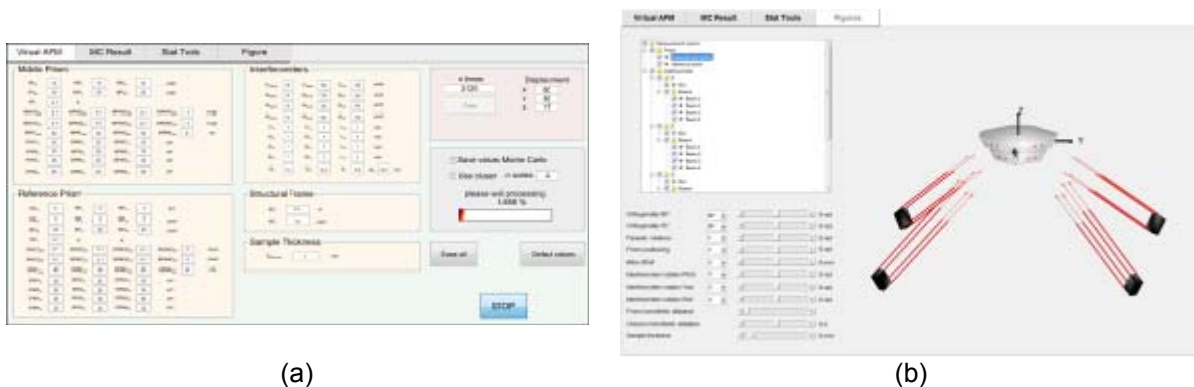


Figure 47: Example of a tipwear curve for a PPP-NCLR cantilever

Virtual SPM

Now that nanotechnology is expanding fast, the precision of measurements achieved at nanometre scale becomes an essential issue to improve the quality and performance of nanoproducts. The entire traceability route is impacted, from the user's instruments to the reference equipment used to calibrate the standards. For dimensional measurements carried out through scanning probe microscopy (SPM) or scanning electron microscopy (SEM), this traceability is achieved thanks to transfer standard (step, grating) whose dimensional properties (height or pitch) have been measured by a reference instrument such as a metrological atomic force microscope (mAFM). The delivered reference values are then recorded in a calibration certificate and associated to a measurement uncertainty. The determination of this measurement uncertainty is, of course, crucial to deliver a confidence level of the calibration. It often leads to difficult tasks for the characterisation of a reference instrument. For some specific mAFMs, few uncertainty component evaluations are experimentally impossible. In this case, some state of the art models must be developed to estimate the uncertainty components. Modelling can also be very useful to better estimate and to refine the measurement uncertainty.

In the frame of the JRP 6DoF, we have developed such a model to estimate the measurement uncertainty of the LNE's metrological AFM. More specifically, it allows overcoming some difficulties linked to the estimation of uncertainties when using a complex instrument design where four interferometric measurements are linearly combined to determine the XYZ positions. In such configuration, the measurement uncertainty becomes too complex to be determined manually, analytically or experimentally. The model was developed under Matlab using object-oriented programming in order to be easily reconfigurable. It takes into account the geometry of the instrument's metrology loop and the interferometric measurements. More particularly, it deals with errors induced by geometrical imperfections of the measuring system such as laser beam misalignments, cosine errors, mirror shape or roughness, prisms non-orthogonality, thermal expansion of the metrology frame, thermal expansion of the prism, Abbe errors, 6 degrees of freedom positioning errors and error due to the variation of sample thickness. Each component of the model (mirror, interferometer, beam, stage) can be translated or rotated (6 degrees of freedom) using homogeneous coordinate formalism. In a first step this allows placing the objects with respect to the instrument design but positioning errors can also be introduced to quantify their impact on the measurement. The model integrates about one hundred parameters that allow controlling the geometry of the metrology loop without using analytical formulas and is widely fed with experimental data.



(a)

(b)

Figure 48: Screenshot of the graphical user interface for (a) the Monte Carlo method with the configuration of all parameters and (b) the view of the modelled metrology loop.

A Monte-Carlo method is then used to determine the positioning uncertainty of the instrument by randomly drawing the parameters according to their associated tolerances and their probability density functions. The whole process follows the Supplement 2 to the Guide to the Expression of the Uncertainty in Measurement (GUM). Some advanced statistical tools like Morris' design and Sobol indices are also used to provide a sensitivity analysis by identifying the most influential parameters and quantifying their contribution to the XYZ positioning uncertainty. The user interface for the configuration of the model parameters are shown in figure 48.

The approach validated during the project allowed for the first time the estimation of the positioning uncertainty of the LNE's mAFM to about 6 nm in the worst condition (when the whole measurement volume is used $60 \times 60 \times 15 \mu\text{m}^3$). More important, it allowed identifying the most critical components. For example, Abbe error was the most important contributor with 75% of the uncertainty and the following 25% were attributed to orthogonality errors. The model also made possible the testing of new configurations and improvements of the instrument. It also showed that the positioning uncertainty could be reduced to ± 1 nm by reasonably decreasing the parasitic rotations of the scanning stage to $\pm 2.5 \mu\text{rad}$ and improving the beam alignment with respect to the AFM tip to ± 0.5 mm. The model also established a limit under which the Zerodur prism used as the metrology reference should be calibrated and the position measurements should be corrected.

The results show that the use of a model fed with sufficient experimental data is a crucial tool to determine precisely the measurement uncertainty of LNE's mAFM, even if the instrument design is complex and that some uncertainty components are difficult to evaluate by other approaches (manual or analytical). The model is a great tool for metrologists that are involved in the development of the mAFM or similar precision measuring machines because it provides a more accurate way to evaluate the positioning uncertainty than previously done. It also gives precious information on how the instrument really behaves and about the best strategies to optimise it.

The approach developed in the project (modelling combined with the use of statistical tools) is very powerful and complete. One of its strengths is that the geometry of the modelled system can be easily reconfigured thanks to the object-oriented programming making the model easily transposable to other mAFMs, instruments or systems that possess metrology loops involving interferometers such as CMMs or scanning stages.

Conclusions

Different aspects on long range AFM has been investigated in the project. Tip wear has been measured for different commercial tips using different form, materials and coatings. The measurements were done with variations of the instrument parameters. The results were compiled in a good practice guide.

The open source software GWYDDION, which is used for data processing of AFM data by a large community of users was extended by routines for intelligent scanning. In addition to the regular scanning different forms of scan trajectories also with a non-homogenous density of measurement points together with routines for resampling are supplied. Using these new possibilities measurement times can be reduced

resulting in smaller measurement uncertainty due to lower drift or the possibility to measure larger samples. The routines have been successfully tested using AFM of the project partners.

These developments are supplemented by programming a virtual AFM to calculate the measurement uncertainty of specific measurement sequences. The virtual AFM can also be used to calculate the uncertainty for different scanning modes in a long range AFM.

This research presents the results for the project objective, '*Improvement of the measurement speed of AFM to allow measurements of larger areas and to reduce drift in the instrumentation*' and the target of the research has been met.

3.6 Summary

1.) Development of the world's first deflectometric method for interferometric straightness measurement using TMS. Comparisons with self-calibration measurements shows an agreement inside of 2 nm, where the standard uncertainty of TMS was more than a factor of 2 smaller. This results in a new calibration service for straightness on encoders, line standards and straightness interferometers at PTB, which for the first time allows for a measurement uncertainty below 10 nm.

2.) An interferometer for simultaneous measurements in 6 DoF was developed. Due to the simple optics design possible by the use of a CCD sensor and the large acceptance angle a robust and price sensitive instrument for characterisation and acceptance tests of tool machines is possible. The work was supported by the stabilisation of a DBR laser diode, which achieved a frequency stability on par with a He-Ne laser in a much smaller form factor at a higher level of output power ideal for a multi axes interferometer.

3.) For the first time a calibration and correction scheme for hexapods have been implemented using a CMM. The method measures three balls on the hexapod by a tactile probe. This led to the world's first calibration service of hexapods by METAS.

4.) NPL set up a testbed for the characterization of nanopositioning stages in six degrees of freedom. This allows for the first calibration service of nanopositioning stages by an NMI.

5.) Different techniques for measuring large areas with AFMs have been implemented. A high speed AFM has been characterized on the NPL testbed for corrections to improve bidirectional scans. In a second step, the high speed AFM was upgraded with a multiaxial laser interferometer system. Intelligent algorithms for adapted scanning modes have been tested and implemented in the open source software GWYDDION as well as investigations on minimizing tip wear. Modelling of the measurement uncertainty of AFMs using Monte Carlo methods in a virtual AFM allows to optimize measurement sequences on large areas.

4 Actual and potential impact

Dissemination

Stakeholder interaction

The results of the project are of interest for tool and measurement system manufacturers in ultra-precision engineering as well as manufacturers of measurement systems for acceptance tests on machine tools and hexapods. Many of these European companies developing ultra-high precision dimensional metrology systems and stages are in the list of the stakeholders of this project. Therefore the most important dissemination is achieved by direct contact with the stakeholders. In addition to meetings at conferences and visits in various institutes, presentations have been given in most of the stakeholder companies.

In the area of nanopositioning and AFM the group of manufacturers is smaller. There are some major companies supplying nanopositioning stages like PI, Queensgate and Smaract, who are acting as stakeholders, but there is no large manufacturer of AFM in the EU, so that the project disseminated the results here mainly by papers, at conferences and in an AFM related workshop.

Conferences

For Precision Engineering in Europe, the EUSPEN conferences are key events. Project results have been presented on the conferences 2014 and 2016. A number of presentations were given at the MACROSCALE

and the international scientific colloquium of the technical university Ilmenau. A highlight was the presentation of the straightness measurement results at the general assembly of CIRP, an important organization in the field of precision engineering.

Important conferences for the dissemination to AFM users were the NANOSCALE conference and workshops in UK, France and Czech Republic, as well as the EUSPEN conference.

Workshops

The project results were presented in a workshop at the first day of the EUSPEN conference in Nottingham 2016. The EUSPEN conference provided a platform to reach a large audience. All project partners presented the results of the project to 50 participants mainly from industry.

A workshop regarding laser sources for interferometry was organised by ISI as well as a workshop for AFM users by CMI.

NPL joined the Cambridge University workshop with a talk about dimensional Nanometrology.

Standards

Over the last 36 months, the project has been presented regularly to the members of the EURAMET technical committee for length (TC-L). TC-L is the committee, which includes specialists on dimensional metrology at the European National Metrology Institutes (NMIs). TC-L will provide information on the IND58 results to the non-participating NMIs; and is also responsible for reviewing new measurement services, which will be a result of this JRP.

The results of the projects regarding the CMM based 6DoF calibration and laser tracer measurements were reported to the ISO "Lasertracker Taskforce" and the VDI groups "Production Measurement Technology" and "Coordinate Measurement Equipment".

Results from the work on fast AFM metrology and information about the testbed for nanopositioning devices were reported to the ISO TC201 as well as to the WG2 of ISO 229 as well as to the VDI group "Surface Metrology in the Micro- and Nanometre-range".

The presentations were given with the intention that the new measurement capabilities and methods can be incorporated in running or future standardisation if possible, not to start a new standardisation process.

Publications

One important output is the technical knowledge from the work in the project, which has been carried out. This knowledge was published so that it can be used by interested scientist and technicians

Overall, 27 peer reviewed papers have been submitted to journals and conference proceedings in precision engineering and nanometrology.

Other dissemination

Project results have been presented in different house journals and annual reports of the institutes involved in the project.

Publication for trade journals have been submitted and developments from the project have been presented at three trade fairs and a one conference exhibition

Regular in house workshops have been used to spread information on the project in the metrology institutes itself.

The gained knowledge of different parts of the project is conditioned into Good Practice Guides for information of interested users, which are listed in Section 6 'List of publication'.

Direct project uptakes

The comparison of different straightness measurement systems will help users and manufacturers to find optimal solutions, when designing 2D and 3D measurement systems based on interferometry as well as for encoder based tools.

The project enabled the University Bristol with the help from NPL to improve the imaging quality of the high speed AFM considerably by offline corrections based on the NPL testbed for nanopositioning stages as well as designing and manufacturing a stage for including online metrology. These improvements are already in use by academic cooperation partners of UoB.

The stabilised laser developed by ISI is used in a interferometric feedback system of an electron beam writer of the company TESCAN. E-beam writers are an important tool to manufacture nanostructured devices by direct writing process. They are used to write photomasks for large volume optical and EUV lithography for VLSI devices but also for smaller volume lithography like gratings or integrated optics devices. TESCAN is one of about five major suppliers of e-beam writers in Europe with the main competitors in Japan. Because e-beam writers are working in a vacuum, interferometers are the best choice for positioning feedback. Laser diodes as light sources have the advantage that they are commonly available in the infrared spectral range, where no interaction with the resist used in the lithography process occurs. Therefore ISI transferred their technology developed in the project to stabilise an 1.5 μm DBR laser diode to a absorption line of a gas cell.

The non-equidistant scanning library developed by CMI and NPL allows for significant reduction of necessary scanning time for typical tasks used in dimensional metrology. The library was included in the open source software GWYDDION which is widely used by AFM users worldwide. AFM users will also benefit from the good practice guide developed from various measurements performed in the project.

PTB is adapting the TMS method and the mathematical tools to other machine designs and interferometer designs in a project together with two European companies.

Some of the stakeholders, those who supplied the project with positioning stages, profited directly from the measurement results. This includes Heidenhain, who gets high resolution straightness information on their manufactured encoders, which will be used to optimise the settings of the writing process. METAS has provided their measurements and compensation models on the test hexapods to the project stakeholders PI and Smaract. As the TUIL was working in close cooperation with SIOS the results regarding straightness measurement on 2D-machines are directly usable there. SIOS as manufacturer of the nano-measurement machine, which is especially used as long range AFM with 25 mm by 25 mm range, also benefits from the better knowledge of tip wear and intelligent scanning, as more use cases become possible.

New Measurement services by the NMIs

The main goal of the project beside disseminating the results by publications and presentations to interested precision engineering tool and measurement system manufacturers and users was the establishment of new and the improvement of existing calibrations services. The instrumentation used for high precision position measurements is very sophisticated and complicated to operate. Therefore, especially for smaller companies, it is not very attractive to acquire and set-up their own measurement system. This is also true even for large companies, who do not always have continuous demand for such instrumentation. Therefore metrology institutes like PTB, NPL, LNE and METAS are offering these measurements as a service for the European industry. The project has generated the following new calibration services in the NMIs:

PTB is supplying a calibration service for length on 1D-reference artifacts like line scales, encoders, and laser interferometers as well as scale calibrations on optical plates. These optical plates are used as standards for optical coordinate measurement systems. The highest demand with regard to the measurement uncertainty comes from the photomask for the VLSI lithography, where PTB calibrates scale on reference masks for the "Advanced Mask Technology Center" in Dresden. While straightness is of large relevance to all of these users, PTB so far was not able to provide such calibrations. As orthogonality is of minor interest for photomasks due to the correction method applied on the lithography tool, the project concentrated more on straightness metrology. Additionally the demand for straightness calibrations grows due to the new 1D+ Encoders of Heidenhain, which combine length and straightness measurement capabilities, which are aimed for inclusion in tool machines and coordinate measurement machines with stacked axes. Better metrology in the machines requires better tools for acceptance tests and calibration, which will be in the first place straightness encoders and straightness interferometers. Due to the project results PTB can now supply a straightness calibration service for 1D+ encoders and straightness interferometers systems with uncertainties in the nano-meter region using the TMS method. These calibrations were worldwide so far only available with uncertainties more than 10 times larger. The calibration

of straightness on optical plates and photomasks requires the use of CCD based microscopes. Such a microscope has been acquired and after implementation straightness calibrations will be performed for some already waiting customers.

Hexapods are very complicated devices with regard to calibrations due to the large length and angular motion range. When hexapods are used for adjustment purposes like in telescopes or optical devices no calibration is necessary. But they are more and more used in tool machines and measurement tools. So far the calibrations are done only along linear axes, where interferometers can be applied. The more natural use of laser tracers has limitations, that for smaller to medium devices the uncertainty of the available tracers are too large and the required number of tracers makes the solution uneconomical. METAS has been contacted by two manufacturers asking for calibration services. Due to the work in this project METAS will for the first time provide a calibration service for hexapods worldwide not available so far. The calibration service is not only usable for hexapods but also for devices with stacked linear and rotational axes. This calibration service will reduce the effort and therefore cost for the instrumentation manufacturers to establish the traceability required for quality management. Due to the modelling effort of METAS this calibration data can directly be used to improve the positioning accuracy of the calibrated stages.

There is also no calibration service available for nanopositioning devices. That makes it difficult for users to perform traceable metrology in the nanometer range. In metrology the most prominent metrological use of nano-positioning devices are high resolution microscopes like AFM. An extreme example is the high speed AFM, where scans with different orientations have to stick together. With the setup of the testbed, NPL is now able to supply such calibration service for device manufacturers as well as for end users. Due to the close cooperation with CMI the supplied measurement data can directly be used in GWYDDION for corrections. The work at NPL was supported by PTB due to the development of mono atomic flat surfaces up to 200 μm as a standard for straightness measurements at nanopositioning devices, which can be provided to the users.

In addition to the new calibration services, the results from the project could be used to improve existing services. LNE could reduce measurement uncertainties for calibrations on their metrology AFM. The improved scanning modes by CMI will lead to faster and therefore less drift dependent AFM calibrations at CMI, NPL and LNE. Also the gained knowledge of tip wear of different tips in use also at the NMIs will help to improve the AFM related services around Europe.

As the work in the project was presented in detail to the stakeholders and published, it would be possible for companies to setup such calibration services themselves, if a large demand develops.

Scientific outlook and future impact

For highest precision applications e.g. in VLSI lithography, the demand for increasing accuracy is obvious from the ITRS and Euramet roadmaps. PTB will therefore continue doing further investigations to explore the limits of the TMS method. In a first step a differential angle interferometer will be included in the NMK and more temperature insensitive adjustment units will be developed and tested. The goal is to bring the uncertainties of the TMS straightness measurements below 0.5 nm.

During many discussions at precision engineering conferences and company visits it was made clear that also for tool machines and coordinate metrology, the topic of 'straightness' gets more and more in the focus. The adaption of the mathematics behind TMS applied to encoder based measurement systems could help to improve the situation. In nearly all tool machines with stacked axes the lateral motion of the axes are not detected, so that the accuracy of the machine depends on the reproducibility of the guidance systems. This problem could be solved by using multi-axes encoder systems in combination with corrections based on TMS. But other than in highest precision applications this market is price sensitive, so that such encoder systems need to remain cheap, while signal detection and data processing has to be done for multiple degrees of freedom. Also the external measurement of the angular motion must be possible at lower cost. Hopefully the development of CMOS technology can help in the future.

The 6DoF-interferometer has been shown in exhibitions, which started discussions to generate a product from the prototype applying for a technology transfer project with the startup company MPRO and another larger company. The optics must be optimised by reducing the dimensions to minimise dead paths and increase stiffness. A suitable material reference for the stabilisation of the laser has to be selected and investigated. As readout speed of the CMOS cameras is limited, while still increasing, it will be necessary to

include motion prediction to allow for integration in higher speed stages. Additionally software must be developed to generate standard conforming data processing for acceptance tests on tool machines. Due to the low hardware effort and the large acceptance angles the 6DoF-interferometer has the potential to minimise the hardware and personal costs of machine acceptance tests. MPRO will also use the underlying procedures and electronics of the interference pattern analyses for a small and inexpensive 3D tactile measurement machine.

While the project has developed a method to calibrate hexapods, it will still be necessary to speed up the measurement. Due to accuracy and speed improvements of coordinate measurement machines the situation will become slightly better, but for a desirable much larger speedup new measurement capabilities will be necessary. One way could be the development of smaller more accurate laser trackers, which can make use of the beam directions, so that three tracers could simultaneously follow three targets on the hexapod stage. This requires better multi-axes angular encoders and the use of error separation methods. Another possibility would be the development of interferometer systems with a high acceptance angle of some 10° . There were some approaches published, but there are no measurement uncertainty evaluations published and the effort for the instrumentation is still high. Therefore further ideas and projects will be necessary to further improve the situation.

The guides about AFM tip wear can only be a snap-shot as all the time new tips come to market and also not all material pairs or AFM parameters could be investigated. Therefore it will be necessary to do further investigations on this field.

As the scanning strategies implemented in GWYDDION are open source, the community of the users will be able to further improve the software library based on special cases and combine it with more AFM instruments.

For the use of AFM as a measurement tool in production processes the measurement speedup will be an important issue. While improving the scanning strategy is one aspect, work on parallelisation is still necessary. A virtual AFM is also an important step for including AFM in the ongoing digitalisation under the label "Industry 4.0", by calculating a measurement specific uncertainty.

5 Website address and contact details

A public website for the project is available at: <https://www.ptb.de/emrp/ind58-home.html>

The contact person for the project is Jens Flügge, PTB, jens.fluegge@ptb.de

6 List of publications

1. N. Vorbringer-Dorozhovets, B. Goj, T. Machleidt, K.-H. Franke, M. Hoffmann, E. Manske, Multifunctional nanoanalytics and long-range scanning probe microscope using a nanopositioning and nanomeasuring machine, *Meas. Sci. Technol.* **25** 044006 (2014)
2. P. Klapatek, M. Valtr, L. Picco, O.D. Payton, J. Martinek, Y. Yacoot, M. Miles, Large area high-speed metrology SPM system, *Nanotechnology* **26** (2015) 065501 (2015)
3. H. Bosse, B. Bodermann, G. Dai, J. Flügge, et.al, Challenges in nanometrology: high precision measurement of position and size, *Shaping the future by engineering: 58th IWK, Ilmenau Scientific Colloquium, Technische Universität Ilmenau* (2014)
4. A. Küng, A. Nicolet and F. Meli, A 5 degrees of freedom μ CMM, *Proc of 14 EUSPEN International Conference DubrovnikVI*, 269, (2014)
5. A. Yacoot, Performance verification of a dual sensor stage, *Proc of 14 EUSPEN International Conference Dubrovnik*, P4.38, 309V1, (2014)
6. J. Hrabina, M. Sarbort, O. Acef, F. du Burck, N. Chiodo, M. Hola, O. Cip and J. Lazar, Spectral properties of molecular iodine in absorption cells filled to specified saturation pressure, *Applied Optics*, Vol 53, Issue 31, pp 7435-7441 (2014)

7. P. Ceria, S. Ducourtieux and Y. Boukellal, Development of a virtual metrological atomic force microscope to better estimate the measurement uncertainty using Monte Carlo method, Proc of euspen's 15th International Conference & Exhibition, Leuven, O3.3, 107 (2015)
8. P. Ceria, S. Ducourtieux and Y. Boukellal, Développement d'un microscope à force atomique métrologique virtuel pour mieux estimer l'incertitude de mesure en utilisant la méthode Monte Carlo, Proc of 18ème Forum des microscopies à sonde locale, 11 (2015)
9. P. Ceria, S. Ducourtieux and Y. Boukellal, Estimation of the measurement uncertainty of LNE's metrological Atomic Force Microscope using virtual instrument modeling and Monte Carlo Method, Proc of 17th International Congress of Metrology, article 14007 (2015)
10. N. Vorbringer-Dorozhovets, R. Füll, E. Manske, Ongoing trends in precision metrology, particularly in nanopositioning and nanomeasuring technology, tm – Technisches Messen 2015; 82(7–8): 359–366 (2015)
11. N. Vorbringer-Dorozhovets, E. Manske, Improvement in long term stability of the long range AFMs, Proc. IMEKO XXI World Congress1, p. 866-871 (2015)
12. E. Manske, R. Füll, R. Mastyló, N. Vorbringer-Dorozhovets, O. Birli, G. Jäger, Ongoing trends in precision metrology, particularly in nanopositioning and nanomeasuring technology, tm – Technisches Messen 2015; 82(7–8): 359–366 (2015)
13. N. Vorbringer-Dorozhovets, E. Manske, G. Jäger, Interferometer-based scanning probe microscope for high-speed, long-range, traceable measurements, PAK 2014 Bd. 60, nr 02, s. 069-072 (2014)
14. A. Koppe, Untersuchungen der Abnutzung von AFM-Spitzen, Masters Thesis, <http://www.tu-ilmenau.de/pms/publikationen/nur-studienabschlussarbeiten/> (2015)
15. N. Vorbringer-Dorozhovets, E. Manske, Long term stability of the long range AFMs, <http://www.ptb.de/emrp/ind58-publications.html> (2015)
16. N. Vorbringer-Dorozhovets, E. Manske, New scanning strategies for long distance AFM measurements, <http://www.ptb.de/emrp/ind58-publications.html> (2015)
17. M. Holá, J. Lazar, O. Číp, Z. Buchta, In-beam tracking refractometry for coordinate interferometric measurement, Proc. SPIE 9132, Optical Micro- and Nanometrology V, 91321K (2014)
18. S. Rerucha, A. Yacoot, T. P. Minh, M. Cizek, V. Hucl, J. Lazar, O. Cip, Laser source for dimensional metrology: investigation of an iodine stabilized system based on narrow linewidth 633 nm DBR diode, Meas. Sci. Technol. 28 045204 (2017)
19. P. Köchert, R. Köning, C. Weichert, J. Flügge, E. Manske, An upgraded data acquisition and drive system at the Nanometer, Proc. ASPE, Precision Interferometric Metrology (2015)
20. J. Hrabina, O. Acef, F. du Burck, N. Chiodo, Y. Candela, M. Sarbort, M. Hla, J. Lazar, Comparison of Molecular Iodine Spectral Properties at 514.7 and 532 nm Wavelengths, Meas Science Review, Vol 14, Issue 4, pp 213-218 (2014)
21. P. Ceria, S. Ducourtieux, Y. Boukellal, A. Allard, F. Nicolas, F. Nicolas, Modelling of the X,Y,Z positioning errors and uncertainty evaluation for the LNE's mAFM using Monte Carlo method, Meas. Sci. Technol. 28, 034007, 16pp (2017)
22. A. Küng, A. Nicolet and F. Meli, Calibration and correction of a 6 degree of freedom piezo driven stage, P1.59, Proc of 16 EUSPEN International Conference Nottingham (2016)
23. P. Köchert, Ch. Weichert, S. Strube, R. Köning, J. Flügge, E. Manske, A fully-fibre coupled interferometer system for displacement and angle metrology, P1.59, Proc of 16 EUSPEN International Conference Nottingham (2016)
24. O. D. Payton, L. M. Picco, T. B. Scott, High-speed atomic force microscopy for materials science, International Materials Reviews, vol 61, issue 8, p 473-494 (2016)
25. E. Manske, Ch. Weichert, G. Ehret, Good practice guide for straightness and orthogonality measurements (2016)



26. C. Weichert, H. Bosse, J. Flügge, R. Köning, P. Köchert, A. Wiegmann, H. Kunzmann, Implementation of straightness measurements at the nanometer comparator, CIRP Annals, 65, 1, 507-510 (2016)
27. C. Weichert, P. Köchert, E. Schötka, J. Flügge, A straightness measuring interferometer characterized with different wedge prisms, (2017) approved awaiting publication.